PERIODICITY AND KINEMATICS OF COPPER-PORPHYRY DEPOSITS FORMATION IN THE PACIFIC BELT OVER THE PAST 125 MILLION YEARS [1]

© 2024 A. N. Didenko [1,*], M. Yu. Nosyrev [2,], G. Z. Gilmanova [2,**]**

[1] *Geological Institute RAS, Moscow*

[2] *Yu.A. Kosygin Institute of Tectonics and Geophysics FEB RAS, Khabarovsk*

**E-mail: gin@ginras.ru*

***E-mail: itig@itig.as.khb.ru*

Received April 26, 2024

Revised August 20, 2024

Accepted October 16, 2024

Statistical analysis of the time series of Cu-porphyry deposits in the Pacific belt and their total ore volume formed in the last 125 million years revealed the presence of a (quasi)cyclic component with a period of 26-28 million years, which accounts for 74% of the total amplitude. An inverse correlation has been established between the global spreading rate on the one hand, and the number of Cu-porphyry deposits in the Pacific belt and their productivity on the other, for the last 125 million years. Relative minimums in spreading rates precede relative maximums in the number and total mass of Cu-porphyry deposits in the Pacific belt and are separated from the adjacent peak by 5-10 million years.

During the formation of large and giant Cu-porphyry deposits in the Pacific belt, the rate of change in the convergence angle in the horizontal plane increases in the interaction zone between two tectonic plates. At the same time, the absolute convergence rate can either decrease or increase. According to geological-structural and kinematic data, the magmatism that formed 8 large and giant Cu-porphyry deposits was accompanied by through-crustal disjunctive disturbances associated either with the change from frontal to "oblique" convergence, or with the transition to a transform continental margin regime, or with a reversive change in the direction of subduction related to island arc-continent collision or island arc-oceanic plateau collision.

Keywords: copper-porphyry deposits, Pacific belt, periodicity and kinematics

DOI: 10.31857/S00167770250105e7

[1] Published for discussion purposes . The Editorial Board considers some of the ideas expressed by the authors in this article to be ambiguous, especially in aspects of tectonic interpretations of the corresponding periods of development of different regions where porphyry copper deposits are located. Those wishing to continue the discussion are requested to send letters to the editorial office.

1. INTRODUCTION

As correctly noted in the Preface to the two-volume special issue of this journal dedicated to porphyry and related deposits of Northern Eurasia (Vikentyev, Bortnikov, 2023, 2024): "The economic significance of ore deposits of the 'porphyry family' and related deposits in the modern world is difficult to overestimate." Indeed, copper-porphyry systems are currently the source of 75% of copper, 50% of molybdenum, 20% of gold, almost all rhenium, and a number of other metals in global production.

Porphyry copper systems are defined as large masses (10-100 km^3 and more) of hydrothermally altered rocks. According to data (Singer et al., 2008; Mihalasky et al., 2015), there are about 700 significant Cu-porphyry deposits in the world (Fig. 1a), with a very wide age range, from practically modern (Andean belt, New Guinea, Philippine archipelago) to Paleoarchean (3234 million years - Coppin Gap, Australia), but the age of most of them (525) is Meso-Cenozoic. Most of the latter, almost 400, are located within the Pacific belt (Fig. 1b). It should be noted that according to A.S. Yakubchuk (2024), as of 2022, over 1200 porphyry systems were known.

Cu-porphyry systems, along with calc-alkaline batholiths and volcanic belts, are indicators of magmatic arcs formed above subduction zones of convergent margins of tectonic plates (Richards, 2021; Sillitoe, 2010; 2012; and many others). A notable but small portion of such systems forms during post-subduction, (post)collisional, accretionary, and transform stages of active continental margin development (Khanchuk et al., 2019; Mineral Resources..., 2023; Richards, 2009; etc.). The processes and factors influencing the formation of large and super-large Cu-porphyry systems can be divided into two groups (Richards, 2021):

1) those occurring in the subduction zone of the submerging oceanic plate – its buoyancy, age, temperature, absolute speed and angle of convergence, geodynamic regime during interaction between the submerging and overriding plates;

2) those developing in the overlying asthenospheric mantle wedge of the subcontinental mantle lithosphere and continental crust of the overriding plate – the rate of ascent and fractionation of magmatic melts, emplacement of intrusive bodies, and the type of volcanism in the upper part of the Earth's crust.

Based on these criteria, and by calculating various geodynamic models of subduction, including their combinations, using open-access self-learning artificial intelligence programs (Scikit-learn Machine Learning in Python; https://scikit-learn.org/stable/index.html), predictive models (maps) were created for several highly promising territories for discovering large Cu-porphyry deposits in the Cordilleras of North and South America (Diaz-Rodriguez et al., 2021): 1)

80–60 million years ago – central Alaska, southern Nevada, California, and Arizona (USA); 2) 66–47 million years ago – southern Ecuador and northern Peru; 3) 60–40 million years ago – Southern California (Mexico); 5) 47–27 million years ago – Peru near 7° S; 6) 23–3 million years ago – Chile near 37° S.

The above age intervals of potential large and super-large Cu-porphyry deposits do not suggest any (quasi)cyclicity in their formation. However, earlier N.L. Dobretsov **(** Dobretsov, 1996 **)** suggested that the age of Cu-porphyry deposits "in the Phanerozoic era is characterized by regular periodicity. The most pronounced are the Cenozoic and Late Cretaceous maximums of 2-5, 30, 60, and 110 million years of copper-porphyry mineralization in the Pacific margin and the Caribbean basin... The nature of this almost regular periodicity in metallogenic literature, as far as I know, has not been discussed."

Despite more than a quarter of a century after the publication of N.L. Dobretsov's quoted work, the problem of (quasi)periodicity in the formation of Cu-porphyry deposits has not been resolved, although some studies have attempted to address it. In the article (Cooke et al., 2005), it was noted that more than half of the 25 largest known Cu-porphyry deposits on the Pacific coast of southern North America and South America were formed during three periods: Paleocene-early Eocene, Eocene-Oligocene, and Middle Miocene-Pliocene. In the work (Sharapov et al., 2013), an attempt was made to evaluate the temporal characteristics of ore-magmatic systems on the active margins of the Pacific Ocean, and one of the conclusions of these authors is as follows – "ME *(metallogenic epochs)* have the dimension of periods of ~ 17, 30, 40, 50 million years." Unfortunately, the above-cited work lacks data on which period is characteristic of certain types of ore-magmatic systems. Therefore, the first objective of this study was to analyze the temporal sequence of formation of Cu-porphyry deposits/systems within the active margins of the Pacific belt.

In the collective monograph (Volkov et al., 2014; p. 68), it is noted: "The true zoning of mineralization in the Pacific belt is determined mainly by the fact that pyrite and copper-porphyry series of ore formations are developed predominantly within island-arc terranes and inner (relative to the ocean) parts of marginal-continental volcanic belts. These parts of volcanic belts usually develop inheritedly on island-arc terranes." This work also indicates that large metallogenic zones are, as a rule, accretionary and post-accretionary, superimposed on ensembles of terranes of various genesis, however, the tectonic (geodynamic) specificity of the belt is determined by island-arc terranes and marginal volcanic belts.

According to statistical calculations conducted in the aforementioned work (Diaz-Rodriguez

et al., 2021), the most important factor in the formation of large Cu-porphyry systems in the eastern part of the Pacific belt is the absolute value of convergence velocity. The second most significant factor is the thickness of deep-sea carbonate sediments and the percentage of carbonates in the sedimentary layer of the oceanic crust. An important factor in the formation of Cu-porphyry deposits is also the angle of convergence; as follows from a number of works on the analysis of disjunctive systems at regional and local levels of paleo- and modern active margins, a significant (if not the majority) number of ore systems or their first phases were formed during the transition period from orthogonal convergence to oblique convergence (for example, Khanchuk et al., 2019; Corbett, Leach, 1998; etc.). Therefore, the second objective of the present research was to analyze the kinematic parameters (velocity and angle of convergence in the horizontal plane) of the subducting tectonic plate at the time of formation of the eight largest Cu-porphyry systems within the Pacific belt, whose ages vary from Aptian to Pliocene (Fig. 1b, Table 1).

The selection of Cu-porphyry deposits of active continental margins in the Pacific Belt was made for two interconnected reasons. First, almost 60% of all these deposits are concentrated specifically on the active margins of the Pacific. Second, it is precisely for the Pacific and Paleo-Pacific that the set of kinematic, paleomagnetic, and other data allows for constructing absolute reconstructions and calculating kinematic characteristics for all oceanic plates, including those that have already disappeared. Such calculations are impossible for Cu-porphyry deposits of ancient fold belts currently located in the interior regions of continents, such as the Central Asian, Alpine, Ural in Eurasia, and the Appalachians in North America (Fig. 1a).

2. FACTUAL MATERIAL AND RESEARCH METHODS

2.1. Geological data

The world database of copper-porphyry deposits (Porphyry Copper Deposits of the World: Database And Grade and Tonnage Models) (Singer et al., 2008) was used as the main factual basis for this research, which utilizes 65 parameters to characterize Cu-porphyry deposits (690 deposits in total in this database). Additionally, another source was used - the database on copper-porphyry deposits of the Russian Far East and Northeastern China (Porphyry Copper Assessment of Northeast Asia-Far East Russia and Northeasternmost China) (Mihalasky et al., 2015), which has approximately the same structure as our main source (Singer et al., 2008).

The main purpose of this work is the spatial-temporal analysis of Cu-porphyry deposits in the Pacific rim (Fig. 1b). To determine the position of deposits within the boundaries of tectonic

plates, the Global model by (Argus et al., 2011) was used. This model is employed in the software complex (GPlates..., 2022), which was used to generate the necessary paleoreconstructions by time and to calculate the absolute velocity and angle of convergence in the horizontal plane of oceanic plates subducting under continental ones, on the margins of which Cu-porphyry deposits were formed.

2.2. Time series analysis

All constructions and time series analyses were conducted using the software packages Acycle (Li et al., 2019) and Past (Hammer et al., 2001).

2.2.1. Smoothing of the original non-uniform time series

To smooth the original non-uniform time series and recalculate it into a uniform one, the Savitzky-Golay filter (Savitzky, Golay, 1964) was used, the essence of which is to approximate using the least squares method with a polynomial i degree in the vicinity of each measurement. In this case, m preceding points from the considered measurement are used. The coefficients of the approximating polynomial depend only on the degree of the polynomial and the number of points taken into account during approximation, and do not depend on the measurement values:

$$Y_t = \frac{1}{\Delta t \times h} \sum_{i=0}^{m-1} a_{i \times X_{t-1}},$$

where Y_t is the current value of the estimated time series, X_t is the current unprocessed value of the original time series, Δ_t is the sampling step of values, h is the normalization coefficient, a_i is the coefficient of the approximating polynomial.

In (Kalambet et al., 2017), a comparison of various methods for filtering noise in spectral characteristics (moving average, modified moving average, linearly weighted moving average, spline interpolation, Bezier curves, adaptive smoothing, Savitzky-Golay filtering) was conducted, and it was established that the latter is the best of those based on the moving average technique. The Savitzky-Golay filtering method allows for achieving the greatest noise suppression and effectively eliminates the influence of noise without disrupting the sensitivity range.

In this work, a Savitzky-Golay filter with an 8-point window and a 4th-order polynomial was used to smooth the original series. The method is implemented in the Past software package (Hammer et al., 2001).

2.2.2. Autocorrelation and cross-correlation functions

The calculation of the autocorrelation function was carried out according to (Davis, 1990):

$$r_\tau = \frac{\sum Y_i \times Y_{i-\tau} - \sum Y_i \times \sum Y_{i-\tau}}{\sqrt{[\sum Y_i^2 - (\sum Y_i)^2] \times [\sum Y_{i-\tau}^2 - (\sum Y_{i-\tau})^2]}},$$

where τ is the lag (step) of autocorrelation. The value of the 95% confidence interval was calculated according to (Davis, 1990):

$$\pm 1.76\sqrt{1/(n-\tau+3)}$$

Using the values of the autocorrelation coefficient and the 95% confidence interval, correlograms were constructed in the interval from 1 to $n/2$, where n is the number of observations in the uniform series.

The calculation of the cross-correlation function was also carried out according to (Davis, 1990):

$$r_m = \frac{\sum (X_i - \overline{X})(Y_{i-m} - \overline{Y})}{\sqrt{\sum (X_i - \overline{X})^2 \sum (Y_{i-m} - \overline{Y})^2}},$$

where m is the lag of mutual correlation. The significance of *(t)* coefficient of mutual correlation (cross-correlation) at the 95% level was calculated according to (Davis, 1990):

$$t = r_m \sqrt{\frac{n-2}{1-r_m^2}}.$$

Cross-correlation analysis is the most appropriate methodological approach for comparing two series that have a "shifted" temporal dependence between them.

Both methods are implemented in the software package Acycle (Li et al., 2019), Past (Hammer et al., 2001).

2.2.3. Spectral analysis using Lomb-Scargle periodograms

Parametric spectral analysis was conducted using the algorithm for constructing power spectrum periodograms by the fast Lomb-Scargle transform method (Lomb, 1976; Scargle, 1982). The method is one of the best for finding periodicity in series with irregular sampling and, importantly for interpretation, it is largely analogous to the Fourier power spectral density method.

For pre-centered data Y_k, when $\sum kY_k = 0$, when constructing the Lomb-Scargle periodogram, the power $P(w)$ is calculated over a set of frequencies wi, and the expression for power is:

$$P(w) \cong \frac{|\sum_k Y_k \cos w(t_k - \tau)|^2}{\sum_k cos^2 w(t_k - \tau)} + \frac{|\sum_k Y_k \sin w(t_k - \tau)|^2}{\sum_k sin^2 w(t_k - \tau)},$$

where τ is the time shift that transforms the model into an orthogonal one and makes $P(\omega)$ independent of translation in τ.

Several versions of programs are available for calculating Lomb-Scargle periodograms,

including the software packages Acycle (Li et al., 2019), Past (Hammer et al., 2001).

2.2.4. Spectral Analysis Using Wavelet Transform

In the last 20-30 years, Wavelet analysis has been successfully applied for structural analysis of geological and geophysical time series (Lyubushin, 2007; Prokoph et al., 2000; etc.), as it is better suited than parametric methods for analyzing non-stationary signals, which is exactly the type of signals represented by time series of the number of Cu-porphyry deposits and their total ore volume per unit of time. Wavelet transform does not simply "cut" the studied series into pieces, but extracts components of different scales, and each component is analyzed with the degree of temporal detail that corresponds to its scale. Additionally, it provides the ability to present all periods of interest on a single diagram and resolve the question of even harmonics. By decomposing a time series into frequency-time space, it is possible to determine how dominant regimes change over time (Lyubushin, 2007; Prokoph et al., 2000). Wavelet analysis is becoming a common tool for analyzing localized power changes in various geological and geophysical time series.

The continuous wavelet transform of a signal x(s) is a value depending on two parameters *(t,a), a > 0* :

$$Wx(t,a) = \frac{1}{\sqrt{a}} \int_{-\infty}^{+\infty} x(s)\, \Psi\left(\frac{s-t}{a}\right) ds = \sqrt{a} \int_{-\infty}^{+\infty} x(t+av)\, \Psi(v) dv \ ,$$

where *t* is the moment of time, *a > 0* is the scale parameter or "period". The value $Wx(t,a)$ reflects the behavior of the studied signal in the vicinity of point *t* with a characteristic scale of variations *a* . The purpose of this transform is to construct a 2D space of values of the modulus $\mathrm{Wx(t,a)}$, which gives a visual representation of the dynamics of emergence, evolution, and disappearance of "characteristic periods" in the time series under study. This value strongly depends on the choice of function *Ψ(t)* .

The most popular function *Ψ(t)* when studying geological and geophysical time series is the Morlet wavelet, as it possesses certain optimality properties in finding a compromise between frequency and time resolution (Lyubushin, 2007):

$$\Psi(t) = \frac{1}{\pi^{1/4}} \exp\left(-t^2/2 - i\pi t\right) .$$

When conducting spectral analysis using wavelet transform in this work, the Morlet wavelet was used.

Currently, there is a significant number of programs for spectral analysis using wavelet transformation, including in Acycle (Li et al., 2019), Past (Hammer et al., 2001).

2.3. Kinematic Analysis

In tectonic plate kinematics, absolute and relative movements are used. In the first case, it implies the movement of one plate or their ensemble relative to an absolute coordinate system, for example, in relation to hot spots or hot fields, which is also identical to the definition – relative to the mantle. In the second case, it refers to the displacement of any single lithospheric plate (tectonic block) in relation to another plate (Cox, Hart, 1989; etc.).

In the present study, we are naturally interested in the kinematic characteristics of the subducting plate relative to the "overriding" plate.

The relative movement between any two plates can be described as a rotation around the Euler pole. At any point $P(\varphi, \lambda)$ along the boundary between plate A and plate B, with latitude φ and longitude $\angle$, the linear velocity V of plate A relative to plate B equals:

$${}_AV_B={}_AW_B\times\vec{P},$$

$\vec{P}$ – is the position vector of the point $P(\varphi, \lambda)$ on the boundary, and ${}_AW_B$ is the angular velocity vector or Euler vector. Both vectors are defined from the origin at the center of the Earth. The direction of relative movement at any point on the boundary occurs along a small circle arc around the Euler pole. Segments with relative movement in the direction away from the boundary are subduction zones.

The magnitude, or velocity, of relative motion increases with distance from the pole, as:

$$|{}_AV_B| = |{}_AW_B||\vec{P}|sin\ \gamma,$$

where γ is the angle between the Euler pole (rotation) and a point on the boundary. All points on the plate boundary have the same angular velocity, but the magnitude of linear velocity changes from zero at the rotation pole to maximum at a distance of 90° from it. On the surface of a sphere, all displacements are rotations; they follow along arcs of circles. The shortest distance between two points on a sphere is not a straight line, as on a plane, but an arc of a great circle with a center coinciding with the center of the sphere. All other arcs on the surface of a sphere, whose circle centers are not at the center of the sphere, are called arcs of small circles.

Calculation of kinematic characteristics of tectonic blocks, including plates moving on the Earth's surface, using paleomagnetic and Euler poles, is implemented in several software packages. The most powerful modern open-access software product that allows building paleoreconstructions and calculating kinematic parameters is GPlates software 2.3 (2022), which was jointly developed by scientists from the School of Earth Sciences at the University of Sydney (led by Prof. Dietmar Müller) and the Division of Geological and Planetary Sciences at the California Institute of Technology (led by Prof. Michael Gurnis). Also important is the fact that the GPlates software

package provides the capability to work with, including import and export of, spatially oriented datasets.

Calculation of kinematic characteristics in the interaction zone between oceanic and continental (subcontinental) plates included the following stages:

1) determination of the tectonic plate (Fig. 1b) on which the Cu-porphyry deposit is currently located. For this purpose, the Global Plate Model (Bird, 2003) was used with adjustments according to (Argus et al., 2011);

2) determination of the tectonic plate position at the time of the corresponding deposit formation and calculation of its coordinates by generating paleoreconstructions using data on lithospheric plate topology and their rotation poles (Cao et al., 2022; Müller et al., 2019) in the GPlates software package (2022). The adequacy of paleoreconstructions was controlled using direct paleomagnetic data for rocks identical in geography and age to the deposits;

3) calculation of the convergence rate and angle in the interaction zone between the subducting and overriding plates in the time range of ±5–10 million years from the moment of deposit formation was carried out using the "Kinematics Tool" subroutine in the GPlates software package (2022).

3. RESULTS OF TIME SERIES ANALYSIS OF Cu-PORPHYRY DEPOSITS IN THE PACIFIC OCEAN PERIPHERY

It was mentioned above that there are about 700 Cu-porphyry deposits in the world, with ages ranging from Paleoarchean to modern (Singer et al., 2008; Mihalasky et al., 2015). The active margins of the Pacific Ocean account for 384 deposits, whose ages range from 291.5 million years to the present. The histogram for the deposits of the Pacific Ocean periphery (Fig. 2a) clearly shows that the majority of them fall within the interval from 0 to 125 million years, with approximately the last 75 million years showing grouping into three clusters (0-20, 28-45, and 50-70 million years), while beyond that no particular pattern is observed. Moreover, for the eastern margin of the Pacific Ocean, these three clusters are distinguished not only in time but also in space (Fig. 1b): 1) in the Gulf of California area, a cluster with the highest density of Maastrichtian-Paleocene Cu-porphyry deposits is identified, the largest of which is Safford; 2) in the south and south of the Altiplano plate, a cluster with the highest density of Eocene-Oligocene Cu-porphyry deposits is identified, the largest of which is Chuquicamata; 3) south of the Eocene-Oligocene cluster of South America, a cluster with the highest density of Miocene-Pliocene Cu-porphyry deposits is identified, the largest of which is El Teniente. The presence of two South American clusters was noted in (Sillitoe, 2012).

Deposits of the youngest age group are more widely developed; they are also found north of the Altiplano plate, within the Panama plate, in North America, and in the western Pacific in the Indonesian-Philippine region (Fig. 1b).

Analysis of the distribution of all Cu-porphyry deposits in the Pacific belt by ore volume (Fig. 2b) revealed the presence of two groups. The first group consists of 112 deposits with ore volumes up to 1 million tons each and ages ranging from virtually modern to 292 million years. The total volume of this group is approximately 56 million tons. The second group consists of 272 deposits with ore volumes ranging from 4.4 to 21,277 million tons and ages also ranging from virtually modern to 282 million years, whose distribution is close to lognormal (Fig. 2b). The total ore mass of the second group is 259,858.8 million tons, which is almost 5 orders of magnitude (4,640 times) greater than the total amount of ore in the first group.

Spectral analysis of the time series of the first dataset through the calculation of Lomb-Scargle periodograms did not show the presence of any significant periodic components - the confidence level of all identified frequencies is significantly less than 50%. Conversely, spectral analysis of the time series of the second dataset showed the presence of three periodic components with confidence levels greater than 50% - approximately 158, 49, and 28 million years, with the confidence level of the latter being very close to 90%.

The distinct (quasi)cyclical nature of Cu-porphyry deposit formation is evident in the "total ore amount - time" relationship. For the original series, in addition to two long-period components (417 and 159 million years), a component with a period of ~27 million years is manifested, which accounts for about 30% in the smoothed series and is distinguished at the 99% probability level (Fig. 2c).

Considering the insufficient initial data on Cu-porphyry deposits of the Pacific subduction belt for the time older than 125 million years (Fig. 2a, c), we limited the interval under consideration and conducted statistical calculations of the original and smoothed time series "total ore amount - time" for 0-125 million years (Fig. 3a).

Autocorrelation analysis of the original series showed that the largest and significant correlation coefficients of the autocorrelation function (Fig. 3b, solid line) correspond to a step of 28 million years (rk=0.408 at a critical value of 0.297 at the 95% confidence level) and a step of 4 million years (rk=0.300 at a critical value of 0.229 at the 95% confidence level). Autocorrelation analysis of the smoothed series (Fig. 3b, dotted line) showed that the largest and significant correlation coefficients correspond to a step of 26-31 million years (highest rk=0.550 at a critical value of 0.302 at the 95% confidence level) and a step of 51-56 million years (highest rk=0.705 at a

critical value of 0.587 at the 95% confidence level). Therefore, according to the autocorrelation analysis data, it can be stated that in the considered time series of the total ore volume of deposits, there is a component with a periodicity of about 26-31 million years. The significant coefficient of the autocorrelation function at a step of 51-58 million years is, with high probability, due to the doubling of the oscillation with a periodicity of 26-31 million years.

On the spectrogram of the original series "total ore amount - time" for Cu-porphyry deposits of the Pacific belt for the last 125 million years (Fig. 3c), it can be seen that the most powerful in magnitude and amplitude is the harmonic with a frequency of 0.0376±0.0011 (25.8-27.4 million years). This harmonic (0.0381±0.0008, 25.7-26.8 million years), exceeding the 99.9% confidence level, is even more clearly distinguished in the smoothed time series of the total ore volume for Cu-porphyry deposits; its value in this time series is more than 74% (Fig. 3d). On the latter spectrogram, the harmonic with a frequency of 0.0381 is the only one possible for interpretation, since the second harmonic, exceeding the 99.9% confidence level, with a frequency of 0.0093±0.0013 (94-125 million years) is comparable in duration to the entire analyzed series. We believe that this component reflects the trend of the entire series, associated with a lower probability of preserving Cu-porphyry systems as a result of secondary, primarily denudation processes.

The next type of spectral analysis that we used is Wavelet analysis. As with the calculation of Lomb-Scargle spectrograms (Fig. 3c,d), both the original and smoothed series were subjected to Wavelet decomposition. In the first case (Fig. 3e), throughout the series with medium intensity, the first oscillation with an average frequency of 0.014-0.017 (60-70 million years) can be traced, and the second with a higher intensity - with an average frequency of 0.03-0.04 (25-33 million years). In the case of the smoothed series (Fig. 3f), the first oscillation with an average frequency of 0.014-0.017 (60-70 million years) practically disappeared, while the second with an average frequency of 0.03-0.04 (25-33 million years) manifested even more clearly over the entire time interval under consideration. As in the case of autocorrelation analysis, we believe that the low-frequency oscillation (60-70 million years) is a doubling of the high-frequency oscillation with a periodicity of 25-33 million years.

In summary of the analysis of temporal distribution of Cu-porphyry deposits in the Pacific belt, it can be concluded that:

a) this series has a (quasi)cyclical component with a periodicity of 26–29 million years (Fig. 3b-e), the proportion of which in the total amplitude of the smoothed series reaches almost 75% (Fig. 3d). Within the Pacific active margin during the past 125 million years, four (2.5–7.5, 31.5–38.5, 53.5–61.5, 85.5–94.5 Ma) and less confidently a fifth (106.5–112.5 Ma) epochs of increased

generation of copper-porphyry deposits are reliably identified (Fig. 2c, 3a);

b) autocorrelation (Fig. 3b) and Wavelet (Fig. 3d, e) analyses revealed another oscillation with a period of ~ 50–70 million years, which is not detected in the Lomb-Scargle spectrograms. We believe it has no geological-geophysical meaning but is a product of slow modulation that occurs for a single-wave mode during the transition to oscillations of doubled period.

4. PALEORECONSTRUCTIONS AND KINEMATIC ANALYSIS OF THE FORMATION TIME OF THE EIGHT LARGEST Cu-PORPHYRY SYSTEMS IN THE PACIFIC BELT

For completeness and objectivity in examining the kinematic characteristics of plate interactions at whose boundaries the largest copper-porphyry deposits form, we selected 8 objects that meet the following conditions: 1) the total tonnage of the deposit exceeds 1 billion tons of ore, meaning all of them, according to the classification (Rundkvist et al., 2004), fall into the category of super-large and giant; 2) well-dated age of the magmatic rocks with which these largest deposits are associated; 3) the age of the object must be within the identified intervals of increased generation of copper-porphyry deposits of the Pacific active margin (see above). Since the geodynamics and kinematics of oceanic plate subduction processes under continental plates on the western and eastern margins of the Pacific Ocean differ significantly, which is confirmed by both model and experimental data (Nagel et al., 2008; and many others), we also wanted to maintain equal representation of objects on different sides of the ocean. As a result, 8 objects were selected – four western with ages from 108 to 2.4 million years and four eastern with ages from 89.5 to 5.4 million years (Fig. 1b, Table 1).

4.1. Atlas Deposit

Currently, it is located on the island of Cebu in the Philippine archipelago within the subcontinental Sunda plate, 260 km west of its boundary with the oceanic Philippine plate (Fig. 1b) and represents the Aptian-Albian age group (Fig. 3a). It is genetically associated with the Lutopan quartz-biotite-hornblende diorite massif, which was intruded into the sedimentary rocks of the Pandan Formation, consisting of interbedded sequences of greenish sandstones-siltstones, polymictic conglomerates, carbonaceous argillites, etc. (Rodrigo et al., 2020). By their appearance and composition, the sedimentary rocks of the Pandan Formation can be classified as accretionary prism rocks. According to chemical composition data, the volcanic rocks of the formation show island arc characteristics (Deng et al., 2015). Radiometric dating of samples from the Atlas mining area (cited from Rodrigo et al., 2020) gave the following results: a) using K-Ar and Rb-Sr systems –

108–101 million years; b) using the U-Pb system on zircons from quartz-diorite porphyrites of the Lutopan massif – 109±2 and 108.5 ± 1.6 million years. The total amount of ore in the deposit is more than 1.4×10^9 tons. No other Cu-porphyry deposits of this age range have been found in the Philippine archipelago, but there are 30 deposits with ages ranging from 25 million years to almost present day, with one of them, Tampakan, having a total ore weight of 2.5×10^9 tons.

The geodynamic setting (tectonic position) at the time of formation of the Atlas deposit is defined as an island arc (Mineral Resources..., 2023). According to paleogeodynamic reconstructions based on geochemical and geological-structural data (Deng et al., 2015; Rodrigo et al., 2020), the sedimentary rocks of the Pandan Formation and the volcanics intruded into them were formed in a suprasubduction setting at the boundary of the continental Australian and oceanic Izanagi plates, the Paleo-Pacific according to (Deng et al., 2015; Rodrigo et al., 2020). Until 115 million years ago, the oceanic Paleo-Pacific (Izanagi) plate was subducting under the continental Australian plate, forming the Proto-Philippine island arc. According to (Deng et al., 2015), after 120 million years, rifting processes began to manifest in the back-arc basin between Australia and the arc (Fig. 4a) with the formation of suprasubduction ophiolites, boninites, which are described on Cebu Island, and the formation of the Proto-Philippine marine (suboceanic) plate. At the boundary of 115 million years, the Proto-Philippine arc became wedged, followed by subduction inversion with the formation of a new island arc – (East Philippine-Daito arc). The position of the Atlas deposit reconstructed in this work at the time of its formation ~ 108 million years ago is located at the boundary of the Philippine (Molucca) and Izanagi plates between the Proto-Philippine arc in the north, which had died out by this time, and the active East Philippine-Daito arc in the south, approximately at 5 ° –7 ° degrees south latitude (Fig. 4a), which is more than 15 ° degrees south of its current position. This amazingly agrees with direct paleomagnetic data for the Pandan Formation for the Early Cretaceous, according to which Cebu Island was located at 8 ° degrees south latitude (Pisarevsky et al., 1922; determination No. 363).

Calculation of instantaneous velocities of the Izanagi plate, which subducted in the WNW direction, and the Philippine plate, which moved in the NE direction, indicates oblique subduction of the former under the latter, possibly also a transform boundary between these plates (Fig. 4a). Calculation of kinematic parameters of the Izanagi plate relative to the Philippine plate in the interval of 118-98 Ma (Fig. 4b, Table 1) showed that the convergence angle of the former changed from almost southern (frontal subduction) to eastern (oblique subduction) direction. The angular velocity of convergence was non-monotonic during this time; initially its decrease was insignificant

from 1.55 to 1.4 ° /Ma [2], and then at the boundary of 110-105 Ma (the time of deposit formation), the velocity decreased to 1.05 ° /Ma. The change in the convergence angle in the interval of 110-105 Ma, calculated for the paleocoordinates of the Atlas deposit, was approximately 50 ° counterclockwise (Fig. 4b; Table 1), while the angular velocity of convergence decreased by 0.30 ° /Ma. The reflection of tangential stresses at the boundary of these plates is a left-lateral shear system of NW-SE orientation, passing through the entire Philippine archipelago (Deng et al., 2015; Rodrigo et al., 2020). It probably served as a transport channel for delivering upper mantle melts from the mantle wedge and metal-bearing fluids from the subducted oceanic crust as a result of dehydration of the latter to the upper horizons of the earth's crust.

4.2. Malmyzh Deposit

It is part of the eponymous ore cluster of the Lower Amur mineragenic zone (State..., 2009) and represents the Cenomanian-Santonian group of deposits (Fig. 3a). Currently, the Malmyzh ore cluster is located within the Gorin zone of the Zhuravlevka-Amur terrane of the Sikhote-Alin orogenic belt of the Amur tectonic plate and quite far, more than 1,000 km, from the active margin of the Pacific plate (Fig. 1b). The main volume of the Zhuravlevka-Amur terrane is composed of turbidites of the Early Cretaceous near-continental syn-shear basin (Geodynamics..., 2006). Deposits and ore occurrences of gold-copper-porphyry, gold-quartz types here are associated with porphyry diorites and granitoids of Cenomanian age, which intrude sedimentary rocks of the Gornoprotok Formation (State..., 2009).

The Malmyzh and the adjacent Poni-Mulinsky gold-copper-porphyry ore clusters form an extended zone of north-eastern trending intrusive bodies of diorite-porphyries and granodiorite-porphyries of three generations, attributed to the Cenomanian Miaochan and Lower Amur complexes (State..., 2009). Several studies have also determined the U-Pb age of zircons from intrusive rocks of the Malmyzh and Poni-Mulinsky ore clusters: 1) granitoids of the Malmyzh field – 100-95 million years (Khanchuk et al., 2019); 2) ore-bearing stocks of diorite-granodiorite composition of the Malmyzh ore field – 101-94 million years (Bukhanova, 2020); 3) igneous rocks of the Malmyzh and Poni-Mulinsky ore fields – 101-92 million years (Petrov et al., 2021).

The total weight of ore at the Malmyzh deposit is more than 2.4×10^9 tons. The geodynamic setting (tectonic position) at the time of deposit formation is defined as mixed (Mineral Resources..., 2023). According to A.I. Khanchuk, the deposit formed during the collision of the Kema island arc

[2] 1 ° /million years ≈ 11.1 cm/year

with the eastern margin of Eurasia. No other Cu-porphyry deposits of this or other age ranges have been discovered within the Sikhote-Alin orogenic belt so far. However, the prospects for discovering new Cu-porphyry deposits within the Poni-Mulinsky and Anadjakansky ore clusters located near Malmyzh are assessed as quite high.

According to paleogeodynamic reconstructions based on geological-structural, biostratigraphic, and geochemical data (Geodynamics..., 2006), the sedimentary rocks of the Zhuravlevka-Amur terrane and the magmatic bodies intruded into them were formed within the active margin of the continental Amur tectonic plate, under which the oceanic Izanagi tectonic plate was subducting. It is quite likely that at this moment the prevailing geodynamic environment in the region was the sliding of the Izanagi oceanic plate along the Amur (Eurasian) continental plate, that is, transform margin conditions were realized, as indicated based on geochemical data in (Khanchuk et al., 2019; Petrov et al., 2021). According to (Khanchuk et al., 2016), the dominant transform regime of the Sikhote-Alin continental margin, which began 110 million years ago, was replaced by a subduction regime at the boundary of 95 million years ago. The existence at this time of large-amplitude, more than 1000-1500 km, movements along the continental margin in the northern direction of the Aptian-Albian rocks of the Kema and Kiselevka-Manomin terranes, currently located to the east of the Central Sikhote-Alin fault, (Arkhipov et al., 2019), confirms the existence of a transform margin. The simultaneous action of oblique subduction and large-amplitude translation of the rocks of the terranes indicated above to the north along the Central Sikhote-Alin fault is also quite likely (Fig. 4c).

The position of the Malmyzh deposit reconstructed in this work at the time of its formation ~ 95 million years ago is located in the zone of the active margin of the continental Eurasian tectonic plate, more precisely its part - the Amur, and the oceanic Izanagi at approximately 65° ° north latitude (Fig. 4c), which is almost 15° ° north of its current position (Fig. 1b, Table 1). According to direct paleomagnetic data (Didenko et al., 2023), for rocks of this age from the Zhuravlevka-Amur terrane (Lower Amur complex - an analog of the Miaoching), the territory under consideration was located at 64° ° north latitude, which perfectly agrees with the reconstructed position of the deposit.

Calculation of instantaneous velocities of the Izanagi plate, which was subducting in the WNW direction, and the Eurasian plate, which was moving almost southward, indicates oblique subduction of the former beneath the latter, possibly even a transform active boundary (Fig. 4c). Calculation of kinematic parameters of the Izanagi plate relative to the Eurasian plate in the interval of 107-87 million years (Fig. 4d, Table 1) showed that the convergence angle of the former changed

from NW to almost northern direction. The angular velocity at the beginning of this period was practically constant at about 1-0.9 ° /million years, but after 100 million years ago it began to increase sharply and by the end of the period under consideration was almost 1.7 ° /million years. The change in the convergence angle of these two plates in the interval of 102-92 million years, calculated for the paleocoordinates of the Malmyzh deposit, was approximately 9 ° counterclockwise (Fig. 4d; Table 1), and the increment of the angular velocity of convergence was +0.38 ° /million years. The reflection of tangential stresses at the boundary of these plates is a powerful echeloned left-lateral shear system of NNE orientation: a) the Priamursky fault is part of the Tan-Lu system, which was formed in the Paleozoic and activated during the Late Cretaceous; b) the Central Sikhote-Alin fault is one of the largest in the Far East, which was formed in the pre-Berriasian time, but the main movements along it occurred in the Late Cretaceous. The cumulative shear amplitude is estimated differently - from the first hundreds (Geodynamics..., 2006) to a thousand kilometers, based on data from (Zabrodin et al., 2015). All these powerful shear systems could serve as transport channels for the delivery of upper mantle melts from the mantle wedge and metal-bearing fluids from the subducted oceanic crust as a result of its dehydration to the upper horizons of the earth's crust.

4.3. Pebble Deposit

One of the world's largest, located in southern Alaska at the edge of the North American tectonic plate on the active margin with the Pacific Plate (Fig. 1b) and represents, like Malmyzh, a Cenomanian-Santonian group of deposits (Fig. 3a). Several terranes are distinguished in southern Alaska (from north to south – Farewell, Wrangellia, Peninsula, Chugach, Prince William, Alexander), which accreted to the North American plate in the Mesozoic (e.g., Coe et al., 1985). The Pebble deposit is located almost at the boundary of the Kahiltna sedimentary basin and the Peninsula terrane, genetically associated with the Kaskanak batholith, which intruded into the flyschoid rocks of the Kahiltna Formation. The batholith consists of calc-alkaline granodiorites, to a lesser extent granites and subordinate andesitic intrusions. The U-Pb age of the batholith zircons is determined as 91–89 Ma (Lang et al., 2013).

The geodynamic setting (tectonic position) at the time of deposit formation is defined in (Mineral Resources..., 2023) as an active continental margin, with a total ore weight of more than 7.5×10^9 tons. However, in the work (Olson et al., 2017), the geodynamic setting at the time of deposit formation is defined as an island arc, and the total amount of ore is 10.9×10^9 tons. In

Alaska, 12 other Cu-porphyry deposits are known with ages ranging from 111 Ma to almost modern, the largest of which – Casino – is also of Late Cretaceous age (73 Ma; Mineral Resources..., 2023).

The reconstructed position of the Pebble deposit at the time of its formation ~ 89 Ma ago corresponds to the active margin zone of the continental North American and oceanic Farallon tectonic plates at approximately 73 ° northern latitude (Fig. 5a), which is 13 ° north of its present position (Fig. 1b, Table 1). According to direct paleomagnetic data for the Lower Cretaceous volcanogenic and sedimentary rocks of the Yukon-Koyukuk basin, located approximately 5 ° north of the Pebble deposit, the nearest point of the continental margin in the Cretaceous was in the area of 65-76° northern latitude (Pisarevsky et al., 2022; determinations No. 402, 453, 455), which does not contradict the reconstructed position of the deposit.

Calculation of the instantaneous velocities of the Farallon plate, which was subducting in the NE direction, and the North American plate, which was moving almost westward, indicates an oblique subduction of the former beneath the latter (Fig. 5a). It is also worth noting the presence of the Izanagi-Farallon mid-ocean ridge subducting under the continent at the time of the Pebble deposit formation (Fig. 5a). Calculation of kinematic parameters of the Farallon plate relative to the North American plate in the interval of 99-78 million years (Fig. 5b, Table 1) showed that the convergence angle of the former changed from a latitudinal to NNE direction. The angular velocity at the beginning of this period decreased from 1.3 to 1.1 ° /million years, and in the interval of 95-90 million years sharply increased to 1.4 ° /million years (Fig. 5b). The change in the convergence angle of these two plates in the interval of 95-84 million years, calculated at the paleocoordinates of the Pebble deposit, was approximately 30 ° counterclockwise (Fig. 5b; Table 1), and the increment of the angular velocity of convergence was +0.11 ° /million years.

The reflection of tangential stresses at the boundary of these plates is a powerful, full-crustal, echeloned right-lateral shear system of NE orientation (Lang, Gregory, 2012). The Pebble deposit area is located southwest of the extensive Lake Clark fault and practically on its strike. The Mulchatna fault runs north of the deposit, and the Bruin Bay fault is to the south, which separates the rocks of the Alaska-Aleutian Range from the sedimentary rocks of the Peninsula terrane to the southeast. It is difficult to determine the full displacement amplitude from Cretaceous time along these faults, but according to aeromagnetic survey data (Haeussler, Saltus, 2005), from the Eocene alone it amounted to almost 30 km along the Lake Clark fault. All these powerful shear systems could have served as transport channels for the delivery of upper mantle melts from the mantle wedge and metal-bearing fluids from the subducted oceanic crust, resulting from the dehydration of

the latter, to the upper horizons of the earth's crust.

4.4. Safford Deposit

One of the largest in the world, represents the next age group - Late Cretaceous-Eocene (fig. 3a). Currently, it is located at a short distance from the active boundary between the oceanic Pacific and continental North American tectonic plates (fig. 1b) within the Basin and Range Province. The latter is one of the world's leading copper provinces, where several dozen Cu-porphyry deposits of Late Cretaceous-Early Eocene age are located in the southwestern United States and northwestern Mexico (fig. 1b) with total identified resources, including mined, of more than 200 million tons of copper.

The Safford deposit itself consists of two ore bodies, San Juan and Dos Pobres, located near the boundary between the Basin and Range Province in the southwest and the Colorado Plateau in the northeast. The deposit is genetically associated with monzodiorite porphyry dikes that intruded into the metavolcanics of the Safford group, composed of massive porphyritic basaltic andesites, andesites, and tuff breccias. The thickness of the dikes varies from several centimeters to 60 m, and some of them can be traced up to 3 km along strike, forming up to a quarter of the ore body volume. There are at least two perspectives regarding the age of the Safford deposit. According to the first (Langton, Williams, 1982; Singer et al., 2008), the age of the deposit is determined by the K-Ar method to be in the range of 57-48 million years; according to the second (Russin, 2008), the U-Pb age of zircons from the dikes of the Dos Pobres ore body is 57.3±1.1 million years, and the U-Pb age of zircons from the host andesites is 73.3±1.0 million years.

The geodynamic setting (tectonic position) at the time of deposit formation is defined in (Mineral Resources..., 2023) as an active continental margin, with a total ore weight of more than 7.2×10^{9} tons. As mentioned above, dozens of porphyry copper deposits of Late Cretaceous-Eocene age have been discovered in the region, with all of them being associated with the Laramide orogeny related to flat slab subduction of the Farallon/Vancouver oceanic plate beneath the continental North American plate during the period of ~ 80-55 million years (English, Jonston, 2004; Mars et al., 2019; et al.). The cause of the distinctive Laramide orogeny, during which a significant increase in crustal thickness occurred, is usually attributed to two factors: a) an increase in the westward migration rate of North America due to the opening of the Atlantic Ocean; b) subduction of the hotter and more buoyant crust of the Pacific-Farallon/Vancouver oceanic ridge (Fig. 5b) and the associated Hess or Shatsky oceanic plateau beneath the continent (Liu et al., 2010).

The position of the Safford deposit reconstructed in this work at the time of its formation ~ 57-52 million years ago corresponds to the active margin zone between the continental North American and oceanic Vancouver tectonic plates at approximately 36° ° north latitude (Fig. 5c), which is about 3° ° north of its current position (Fig. 1b, Table 1). According to direct paleomagnetic data for Late Cretaceous-Early Eocene granodiorites and andesites, the Colorado Plateau, located approximately 1.5° ° south of the Safford deposit, was at 35±3° °N at the time of the latter's formation (Pisarevsky et al., 2022; determinations 242, 243, 7483), which agrees perfectly with the reconstructed position of the deposit in this work.

Calculation of instantaneous velocities of the Vancouver/Farallon plate, which was subducting in the ENE direction, and the North American plate, which was moving in the SSW direction, indicates frontal subduction of the former under the latter (Fig. 5c), but calculation of kinematic parameters of the Vancouver/Farallon plate relative to the North American plate in the interval of 63-43 Ma (Fig. 5d, Table 1) showed that the convergence angle of these plates still varied from NE to ENE direction. The angular velocity at the beginning of this period decreased from 1.15 to 0.9 ° /million years, and in the interval of 56-51 Ma sharply increased to 1.3 ° /million years (Fig. 5d). This is consistent with independent data on the convergence rate of the Farallon and North American plates during the Laramide orogeny (English, Johnston, 2004), according to which it could reach 15 cm/year. The change in the convergence angle of these two plates in the interval of 56-51 Ma, calculated for the paleocoordinates of the Safford deposit, was 30 ° clockwise (Fig. 5d; Table 1), and the increment of angular convergence rate was +0.42 ° /million years.

The San Juan, Dos Pobres, and other ore bodies are localized in numerous sublatitudinal, NE and NW normal faults associated with basement uplifts during the Laramide orogeny and extending to the boundary between the lithospheric mantle and the Earth's crust (English, Jonston, 2004; Mars et al., 2019; etc.). The vertical amplitude of one of these NW faults cutting through the Dos Pobres ore system is ~ 1 km. Probably, these fault zones served as transport channels for the delivery of upper mantle melts from the mantle wedge and metal-bearing fluids from the subducted oceanic crust as a result of its dehydration to the upper horizons of the Earth's crust. It should be noted that the formation of the Safford deposit occurred during the final stage of the Laramide orogeny (the end of the flat subduction stage of the Farallon/Vancouver plate under the North American plate) or even somewhat after its completion.

4.5. The Chuquicamata Deposit

One of the world's largest deposits by total ore volume, exceeding 21 billion tons (Mineral Resources..., 2023), represents the next age group - Eocene-Oligocene (Fig. 3a). In this same age group and cluster, there are at least 23 other large Cu-porphyry deposits (Fig. 1b), with 12 of them having total ore reserves exceeding 1 billion tons: Escondida, El Salvador, Gaby, Collahuasi, and others. Currently, Chuquicamata is located near the active boundary between the oceanic Nazca plate and the continental South American plate (Fig. 1b).

The Chuquicamata deposit is genetically linked to the Chuqui intrusive complex, composed of porphyritic granodiorites and monzogranites of several large massifs - Eastern, Western, Banco, and others, which can be traced for more than 30 km along a powerful submeridional fault zone called the West Fault, which is part of the major Domeyko fault zone, along which other large porphyry clusters are located (for example, Escondida). On the east, the Chuqui complex is framed by metamorphosed dacites, rhyodacites, granodiorites of Triassic and Paleozoic age, and on the west - by sandstones of the Lower Cretaceous San Salvador Formation, Eocene andesites of subduction genesis, and Eocene-Oligocene diorites and granodiorites of the Los Picos and Fortuna complexes (Ossandon et al., 2001). Analysis of numerous geochronological materials, including unpublished ones, allowed (Ossandon et al., 2001) to draw the following conclusions: 1) The Eastern ore body is probably older than the Western one, but both were formed before 33 million years (U-Pb age of zircons from the Eastern, Western, and Banco ore bodies is 34.8±0.3, 33.3±0.3, 33.4±0.4 million years, respectively); 2) the main stage of hydrothermal activity followed approximately 2 million years later as a separate event (40Ar/39Ar age of sericite 31.1±0.2 million years). According to (Singer et al., 2008), the age of the deposit is determined to be in the range of 35-31 million years.

The geodynamic setting (tectonic position) at the time of deposit formation was defined in (Mineral Resources..., 2023) as an active continental margin. As mentioned above, dozens of Eocene-Oligocene copper porphyry deposits have been discovered in the region, with all of them associated with an episode of "flat slab subduction" of the Farallon oceanic plate under the continental South American plate (Ramos, Folguera, 2009), similar to the Laramide orogeny episode in the southern regions of North America. This Late Eocene-Oligocene episode of flat subduction at the active margin of the South American plate received its own name – Altiplano (Ramos, Folguera, 2009).

The position of the Chuquicamata deposit reconstructed in this work at the time of its formation ~ 33 million years ago corresponds to the zone of the active margin of the continental South American tectonic plate and the oceanic Farallon plate at approximately 26° ° south latitude

(Fig. 6a), which is approximately 5° ° south of its current position (Fig. 1b, Table 1). There are no direct paleomagnetic data for the time of deposit formation. For this region, there is only a determination based on Oligocene sediments, according to which at the boundary of 23–26 million years ago, the Chuquicamata deposit was located at 22.2±3.4° ° south latitude (Pisarevsky et al., 2022; determination 8421), which agrees well with the reconstructed position of the deposit (Fig. 6a).

Calculation of instantaneous velocities of the Farallon plate, which was subducting in the eastern direction, and the South American plate, which was moving in the WNW direction, most likely indicates a frontal subduction of the former under the latter (fig. 6a), as the horizontal convergence angle of these plates was more than 60° (table 1). However, the calculation of kinematic parameters of the Farallon plate relative to the South American plate in the interval of 43–23 million years (fig. 6b, table 1) showed that the convergence angle of these plates still varied from NE to ENE direction. The angular velocity at the beginning of this period increased from 1.15 to 1.65 ° /million years, and after 33 million years sharply decreased to 1 ° /million years (fig. 6b). The change in the convergence angle of these two plates in the interval of 35–30 million years, calculated on the paleocoordinates of the deposit, was about 10 ° clockwise (fig. 6b; table 1), while the angular velocity of convergence decreased by 0.30 ° /million years.

As mentioned above, the main ore bodies of the deposit are traced for more than 30 km along a powerful submeridional fault zone called the Western Fault. The latter is part of the regional right-lateral strike-slip Domeyko system, stretching for several hundred kilometers in the meridional direction along the Cordilleras (Amilibia et al., 2008) and hosting, besides Chuquicamata, other giant Cu-porphyry deposits – Escondida, El Salvador, Gabu, Collahuasi. According to (Mpodozis, Cornejo, 2012), the deep strike-slip Domeyko system served as the main transport channel for the delivery of upper mantle melts from the mantle wedge and metal-bearing fluids from the subducted oceanic crust as a result of its dehydration to the upper horizons of the earth's crust.

4.6. El Teniente deposit

In the following Late Miocene-Pliocene age group, El Teniente is one of the largest deposits (fig. 3a). In the same age group and in the same cluster, there are several other large Cu-porphyry deposits – Los Bronces, Los Pelambres, Vizcachitas, etc. This age group also includes several dozen Cu-porphyry deposits on the other side of the Pacific Ocean from Oceania in the south to the Philippines in the north (fig. 1b).

El Teniente is located on the active boundary between the oceanic Nazca and continental South American plates (1b) in the Main Cordillera zone of the Chilean-Argentine Andes. It is genetically linked to dikes of porphyry dacites and latites, collectively known as the Teniente plutonic complex (Stern et al., 2011). The rocks of the latter are intruded into the Early Miocene-Early Pliocene volcanics of the Farallon formation – products of the marginal volcanic belt. The El Teniente deposit itself is a volcanic crater (Braden breccia pipe), penetrated by ring dikes 6-8 m thick of porphyry dacites and latites, with U-Pb zircon ages of 5.8-4.8 million years (Maksaev et al., 2004; Stern et al., 2011). The age of the deposit according to (Mineral Resources..., 2023; Singer et al., 2008) is determined in a wider interval – 6.3-4.4 million years.

The geodynamic setting (tectonic position) at the time of deposit formation is defined in (Mineral Resources..., 2023) as an active continental margin. It was mentioned above that in the same age group and in the same cluster there are several other large Cu-porphyry deposits, with total ore reserves exceeding 47 billion tons (Singer et al., 2008). The formation of deposits in this cluster is also associated with the episode of "flat slab subduction" of the oceanic Nazca plate under the continental South American plate, similar to episodes of the Laramide orogeny in the southern regions of North America and Altiplano in the Central Andes. This Late Miocene-Pliocene episode of flat subduction on the active margin of the southern South American plate, which occurred approximately 13-5 million years ago, received its own name – Poyenia, after the volcanic province of the same name (Ramos, Folguera, 2009; 2011).

The reconstructed position of the El Teniente deposit at the time of its formation ~ 5.4 million years ago corresponds to the active margin zone of the continental South American tectonic plate and the oceanic Nazca plate at 35° ° south latitude (Fig. 6c), which approximately coincides with its current position (Fig. 1b, Table 1). For the Miocene volcanics of the Farallon Formation, which hosts the ore bodies, there is a paleomagnetic determination according to which in the Late Miocene the region was located at 36° ° south latitude (Pisarevsky et al., 2022; determination 8472), which is consistent with the reconstructed position of the deposit (Fig. 6c).

The calculation of instantaneous velocities of the Nazca plate, which was subducting in the ENE direction at high speed, and the South American plate, which was moving almost northward at low speed, indicates, most likely, the beginning of oblique subduction of the former under the latter (Fig. 6c). The calculation of kinematic parameters of convergence of these plates in the interval of 15–0 million years (Fig. 6g, Table 1) showed that the convergence angle of these plates changed little – from 87° ° to 77° ° , but the angular velocity since the beginning of this period decreased

from 1.2 to 0.8° ° /million years (Fig. 6g). The change in the convergence angle of these two plates in the interval of 8–3 million years, calculated for the paleocoordinates of the deposit, was 10° ° counterclockwise, while the angular velocity of convergence decreased by 0.10° ° /million years. (Fig. 6g; Table 1)

The El Teniente deposit is entirely located at the intersection node of the regional Teniente fault zone of NE-SW direction and the Puquios-Codegua fault of NW-SE direction (Stern et al., 2011), which probably served as transport channels for the delivery of upper mantle and subducted material to the upper horizons of the earth's crust.

4.7. Panguna Deposit

Located on one of the Solomon Islands - Bougainville (Papua New Guinea) in the active boundary zone between the Pacific oceanic plate and the Solomon Sea microplate, which belongs to the continental Australian plate (Fig. 1b). Bougainville Island is part of the Melanesian island arc formed as a result of calc-alkaline subduction magmatism during the Eocene-Late Miocene. The host rocks of the deposit are Late Miocene-Early Pliocene porphyry andesites of the Kieta volcanic complex, and the deposit itself is genetically associated with multi-phase intrusive bodies of Kawerong quartz diorites. The age of the earliest stage (K-Ar) is 4-5 million years, and the mineralized and highly altered intrusive bodies have an age of 3.4 ± 0.3 million years (Eastoe, 1979; Page, McDougal, 1972). The latter is interpreted as the age of mineralization of the Panguna formation rocks and is indicated in (Mineral Resources..., 2023; Singer et al., 2008).

The geodynamic setting (tectonic position) at the time of deposit formation is defined in (Mineral Resources..., 2023) as an island arc, and the total weight of ore is more than 1.4×10^{9} tons. The reconstructed position of the Panguna deposit at the time of its formation ~ 3.4 million years ago corresponds to the active Melanesian island arc zone at the boundary of the oceanic Pacific plate and the Solomon Sea microplate at 6.7 ° south latitude (Fig. 7a) and practically corresponds to its current position (Fig. 1b, Table 1). For the Miocene-Pliocene calcisiltites of one of the Solomon Islands (Malaita Island), there is a paleomagnetic determination (Musgrave, 1990), according to which in the Late Miocene the region was at 7.9 ° south latitude (Pisarevsky et al., 2022; determination 6578), which is consistent with the reconstructed position of the deposit (Fig. 7a).

Calculation of instantaneous velocities of the Pacific Plate, which migrated in a WNW direction at high speed, and the Australian Plate, which moved in a NE direction also at high speed, indicates most likely an active transform boundary between these plates (Fig. 7a). Calculation of

kinematic parameters of the Pacific Plate relative to the Australian Plate in the interval of 10–0 million years (Fig. 7b, Table 1) showed that the convergence angle of these plates changed insignificantly – from 257 ° to 250 ° , the angular velocity since the beginning of this period also decreased slightly from 1.10 to 1.09 ° /million years (Fig. 7b). The change in the convergence angle of these two plates in the interval of 6–2 million years, calculated for the paleocoordinates of the deposit, was about 7 ° counterclockwise, while the angular velocity of convergence decreased by only 0.01 ° /million years. (Fig. 7b; Table 1). It should be noted that a rather sharp change in the direction of the convergence angle 6 million years ago (Fig. 7b) correlates in time with the beginning of the change in the direction of subduction in the Late Miocene; if before this time the Pacific Plate subducted under the Australian Plate, then subsequently the opposite occurred – the Australian Plate began to subduct under the Pacific Plate. This could have been caused by the jamming effect of the Ontong Java Plateau (Hackman, 1980; Taylor, 1987).

A distinctive structural feature of the Solomon Islands archipelago is the numerous faults predominantly of NW and NNW strike. One of them, located on the coast of the Solomon Sea to the southwest of the deposit, can be traced for a distance of more than 100 km and is probably part of a regional NW fault system separating the Central "sedimentary" and Pacific "volcanic" provinces of the Solomon Islands (Coleman, Hackman, 1974). In the area of the deposit itself, there are faults of both NW and NE strikes (Geological map..., 1967), which probably served as transport channels for the delivery of upper mantle and subducted material to the upper horizons of the earth's crust.

4.8. Grasberg Deposit

This unique Au-Cu-porphyry deposit with a total ore volume of 7.5×10^{9} tons began to be developed in 1989 and for many years remained the first in gold production and third in copper production worldwide. The deposit is located on the island of New Guinea (Indonesia) in the active boundary zone between the Caroline oceanic plate and the Maoke microplate, which belongs to the continental Australian plate (Fig. 1b). The deposit is genetically linked to a three-phase intrusive complex: 1) the earliest Dalam phase, composed of diorites and andesites; 2) the main phase, Grasberg proper, composed of porphyritic quartz monzodiorites; 3) the third Kali phase, composed of quartz monzodiorite dikes. The K-Ar and Ar-Ar ages of the porphyritic quartz diorites of the main phase are 3.2–2.8 and 3.3–3.0 million years, respectively (Paterson, Cloos, 2005). The age of the deposit according to (Mineral Resources..., 2023) is defined as Pliocene. The rocks hosting the intrusive complex are Eocene-Oligocene sedimentary formations of the New Guinea group

(Paterson, Cloos, 2005).

The geodynamic environment (tectonic position) at the time of deposit formation is defined in (Mineral Resources..., 2023) as postconvergent, which could have been realized after the cessation of subduction and the collision of an island arc with a continent or oceanic plateau. Probably, one of the reasons for the formation of the Grasberg deposit was the collision of an island arc with the Australian plate during the Late Miocene-Pliocene (Paterson, Cloos, 2005). Such collisions lead to changes in arc polarity.

The position of the Grasberg deposit reconstructed in the present work at the time of its formation ~ 3 million years ago corresponds to the active boundary zone between the continental Australian and oceanic Caroline plates at 5 ° –6 ° degrees south latitude (Fig. 7a) and practically corresponds to its modern position (Fig. 1b, Table 1). According to paleomagnetic data for Miocene volcanics of Papua New Guinea island, the paleolatitude of the Grasberg deposit formation was in the range of 1-5° south latitude (Pisarevsky et al., 2022; determinations 1911, 1912).

The calculation of instantaneous velocities of the oceanic Caroline Plate, which migrated almost northward, and the continental Australian Plate, which moved northeastward onto the Caroline Plate (Fig. 7a), is consistent with the assumed island arc-continent collision. The calculation of kinematic parameters of the Caroline Plate relative to the Australian Plate in the interval of 10-0 Ma (Fig. 7b, Table 1) showed that the convergence angle of these plates at the boundary of 5 Ma began to change sharply - by more than 80 ° counterclockwise, and from the same time, the angular velocity sharply increased from 1 to 1.9 ° /Ma (Fig. 7b). The change in the convergence angle of these two plates in the interval of 5-0 Ma, calculated on the paleocoordinates of the deposit, was about 85 ° counterclockwise, while the angular velocity of convergence also increased significantly - by 0.87 ° /Ma. (Fig. 7b; Table 1). It should be noted that the sharp change in the direction of the angle and speed of convergence of these two plates 5 Ma ago lags somewhat behind the beginning of magmatic activity associated with the collision stage - 7.1-2.5 Ma (Paterson, Cloos, 2005).

The Grasberg deposit is entirely located at the intersection node of two regional fault systems: 1) the WNW-ESE system includes powerful left-lateral strike-slip faults - Wanagon, Ertsberg 1 and 2, Heat, Meren; 2) the SW-NE system also includes left-lateral strike-slip faults Grasberg, Carstensz, New Zealand. Probably, these fault systems served as transport channels for the delivery of upper mantle and subducted material to the upper horizons of the earth's crust. It has been established (Sapiie, Cloos, 2004) that the placement of ore-bearing intrusions was controlled

mainly by tectonic movements generating space, rather than by the pressure of the intruding magma.

5. BRIEF DISCUSSION

The discovery of large and super-large Cu-porphyry deposits requires significant investments in both time and material resources. Statistically, only one out of every thousand explored Cu-porphyry occurrences becomes a major mine (Richards, 2021). As evident from numerous works and the material presented above, large and super-large Cu-porphyry deposits form spatial-temporal clusters, meaning that, most likely, there is a global structural heterogeneity, a key to understanding how and why they accumulate in these particular places rather than others. Explaining this heterogeneity is of fundamental importance for predicting regions with Cu-porphyry systems. In the material presented above in two sections, an attempt has been made to examine the patterns (or heterogeneities) in the distribution of Cu-porphyry deposits of the Pacific belt in time and space.

As previously indicated, the processes and factors influencing the formation of large and super-large Cu-porphyry systems can be divided into two groups. The place of the first group is the subduction zone of the descending plate, while the second includes the overlying asthenospheric mantle wedge, subcontinental mantle lithosphere, and continental crust of the overriding plate. According to Richards (2021), there are 9 main factors determining the existence of an economically viable Cu-porphyry deposit: from the subduction of oxidized hydrated oceanic lithosphere to uplift and erosion with exposure of the subvolcanic level.

5.1. Analysis of kinematic characteristics

At the beginning of the discussion, we will examine materials on kinematic analysis and paleogeodynamic reconstructions for the eight largest deposits in the belt. From these data, we can make three very important assumptions, as we see it, about the dynamic processes (phenomena) that significantly influenced the productivity of the deposits under consideration.

During the formation of eight large and giant Cu-porphyry deposits of the Pacific belt, there is an increase in the rate of change of the convergence angle in the horizontal plane of two interacting tectonic plates (Table 1; Fig. 4b, d, 5b, d, 6b, d, 7b, c). In some cases, this rate can reach very significant values, almost up to 1°/million years, while the absolute convergence velocity can either decrease or increase (Table 1). The calculations carried out in this work fully agree with the statement (Diaz-Rodriguez et al., 2021; Richards, 2021) that the high convergence rate in the interaction zone of oceanic and continental tectonic plates is the most important feature associated with the formation of Cu-porphyry systems. The convergence rate controls the volume of material subducted into the upper mantle, including carbonate rocks in the upper volcanic part of the oceanic

crust and water-rich pelagic deep-sea sediments, which increase the metasomatic enrichment of the mantle wedge with volatile substances, sulfur, molybdenum, gold, large-ion lithophile elements and, ultimately, contribute to the formation of Cu-porphyry systems in the overlying continental plate.

Immediately before the formation of each of the eight deposits considered, there was a rather sharp change in the direction of convergence in the horizontal plane (Table 1; Fig. 4b, d, 5b, d, 6b, d, 7b, c), which was accompanied either by a change from orthogonal convergence to oblique convergence (Corbett, Leach, 1998; et al.), or by a transition to a transform continental margin regime (Petrov et al., 2020; Khanchuk et al., 2019; et al.), on the one hand. On the other hand, the change in the direction of convergence should have led to differential rotations of individual blocks and the formation of crustal-scale disjunctive disturbances. According to literature data and our own (Malmyzh deposit) geological and structural data, considered in the previous section, the volcano-plutonic magmatism, which resulted in the formation of 8 large and giant Cu-porphyry deposits, was accompanied by crustal-scale disjunctive disturbances, often echeloned. According to (Richards, 2021; et al.), these systems of orogen-parallel strike-slip faults in transpressive tectonic conditions serve as pathways for magma ascent from deep reservoirs to the upper layers of the earth's crust, limiting direct hydraulic connection with the surface and promoting the predominance of plutonism over volcanism.

In (Mineral Resources..., 2023), the tectonic settings for the formation of the eight deposits considered are defined as follows (Table 1, column 1): island arc – Atlas, Panguna; continental margin – Pebble, Safford, Chuquicamata, El Teniente; post-convergent – Grasberg; and mixed – Malmyzh. The paleogeodynamic reconstructions built in this work and their analysis allow us to state that these definitions are too general and sometimes unclear, for example, for the Malmyzh deposit. As follows from the analysis of reconstructions (Fig. 4a, c, 5a, c, 6a, c, 7a) and generalizations made on their basis (Table 1, column 10), an unambiguous definition of the geodynamic (tectonic) setting is hardly possible.

On the western edge of the Pacific Ocean, in three of the four examined examples, deposit formation was accompanied by collision of island arcs with continental plates, with the exception of Panguna where an island arc collided with the Ontong Java oceanic plateau. Here, the "old" oceanic lithosphere (far from mid-ocean ridges) with relatively high average density subducts into the mantle beneath continents, forming systems of island arcs, inter-arc and back-arc basins. On the eastern edge of the ocean, the situation is different. Here, firstly, the formation of three of the four examples considered (with the exception of Chuquicamata) was accompanied by subduction of mid-oceanic and aseismic ridges or plateaus under the continent. Secondly, again, the formation of three

of the four examples considered (with the exception of Pebble) occurred against the background of different stages of flat subduction and associated orogenies – Laramide for Safford, Altiplano for Chuquicamata, and Payenia for El Teniente. In this part of the Pacific belt, "young" and relatively hot oceanic lithosphere (mid-ocean ridges nearby) with relatively low density and high buoyancy subducted at a shallow angle under the western American continental margin, where compression occurred in the rear of the volcanic belt that was retreating toward the continent.

A direct correlation between magmatism that enabled the formation of Cu-porphyry deposits on one hand, and flat subduction on the other, is hardly possible. Periods of flat subduction are usually considered amagmatic (for example, Humphreys et al., 2003). Studies (Kay et al., 2001; Ramos, Forguera, 2009) show that Miocene Central Andean ore districts (22°–34° south latitude) have common tectonic and magmatic features that indicate their formation in a flat subduction zone or during the initial increase of the subduction angle in previously flat subduction zones. The timing of deposit formation usually corresponds to peaks of crustal deformation, which roughly coincide in time along the Andean front from Peru to Chile and occurred during periods of westward rollback of the subducting Nazca plate relative to South America. It is more accurate to say not "plate rollback" but "slab hinge rollback." Such a regime may be associated with changes in plate direction and spreading rate, which is particularly clearly recorded for the time of formation of the Safford deposits (Fig. 5d) and Chuquicamata (Fig. 6b). We believe that the magmatism associated with Cenozoic Cu-porphyry deposits on the western coast of America occurred either during brief periods of slab hinge rollback of the subducting Farallon and Nazca plates, or in immediate temporal proximity to the onset of the next stage of flat subduction. According to the latest model (Fig. 3 and corresponding text from Kay et al., 2001), the Late Miocene-Pliocene cluster of Cu-porphyry deposits (El Teniente, Los Bronces, Los Pelambres, Vizcachitas, etc.) on the western coast of South America (Fig. 1a) formed by 6.5 million years ago, while the cessation of magmatic activity, associated with the episode(s) of flat subduction of Poyenia or Pampea, occurred around 3 million years ago. The age of the deposits according to (Mineral Resources..., 2023; Singer et al., 2008) is determined in a broader interval – 6.3–4.4 million years.

Analysis of constructed reconstructions and kinematic parameters of interacting plates allows to conclude that the formation of eight large and giant Cu-porphyry deposits of the Pacific belt occurred during major tectonic events at the boundary of oceanic and continental plates - collisions of island arcs with continental plates, subduction of oceanic plateaus and ridges under continental plates, and changes in subduction direction. Another important conclusion that follows from the text of this section is a significant increase in the thickness of the Earth's crust in regions with Cu-

porphyry deposits, which occurred both due to the collision of island arcs and subduction of oceanic plateaus and ridges, as well as flat subduction. The latter is characteristic only of the western coast of North and South Americas in the post-Cretaceous period.

5.2. Analysis of the time - Cu-porphyry deposits relationship for the Pacific belt

When analyzing time series of the number and volume of Cu-porphyry deposits in the Pacific belt in the interval of 125-0 million years, a (quasi)cyclic component with a periodicity of 26-29 million years was identified (Fig. 3b-e), the share of which in the total amplitude of the smoothed series reaches almost 75% (Fig. 3d). According to literature data, almost identical periodicities in the Meso-Cenozoic have been identified for time series of a significant number of global characteristics: 1) extinction episodes of both marine - 26 million years (Raup, Sepkoski, 1984; etc.) and non-marine - 27.5 million years (Rampino et al., 2021a) organisms; 2) major/global geological events, including extinction of organisms, oceanic anoxic events, manifestations of plume magmatism, changes in ocean level, reorganization of tectonic plate migration, etc. - 26.9 million years (Rampino et al., 2021b); 3) spreading rates - 27.3 million years (Boulila et al., 2021; Muller et al., 2019).

Naturally, the discovery of a periodic component in the time dependence of the total ore volume of Cu-porphyry deposits in the Pacific Belt, identical in duration to one of the components in the time dependence of the spreading rate, prompted us to conduct a more detailed comparison of these characteristics. The upper part of Fig. 8a shows the original time series of spreading rate (Muller et al., 2019) and its general trend (Boulila et al., 2021) in the interval of 0-125 million years. The lower part of Fig. 8a shows the time series of spreading rate after trend removal (line 3) and the model series of its largest harmonic (line 4), with a frequency value of 0.038±0.006. Fig. 8b in the upper part shows the original series of the total ore volume (line 5) and the smoothed Savitzky-Golay filter (line 6). In the lower part of the same figure, the model reconstructed time series of the total ore volume (line 6) and its largest amplitude harmonic (line 8) are presented, with a frequency value of 0.038±0.001.

Comparison of the graphs described above (Fig. 8, gray rectangles) showed a very clear correlation for five extremes on each of these dependencies; relative maximums on curve No. 8 correspond to relative minimums on curve No. 4. As can be seen, the relative minimums in the time dependence of the spreading rate slightly precede the relative maximums in the time dependence of the total ore volume.

Let us recall that, according to statistical calculations from the work of (Diaz-Rodriguez et

al., 2021), the most important factors in the formation of large Cu-porphyry systems in the eastern part of the Pacific Belt are the absolute value of the convergence rate and the thickness of deep-sea carbonate sediments, the percentage of carbonates in the sedimentary layer of the oceanic crust. We believe that the relationship discovered in this work between the spreading rate, on the one hand, and the total ore volume of Cu-porphyry deposits, on the other, can be explained as follows. *Decreasing spreading rate contributes to increased volume of oceanic plate material (Zhou et al., 2020) subducting into the upper mantle, including carbonate phases, water-rich pelagic deep-sea deposits, and serpentinized mantle, which, when subducting under continental plates, enhance the transfer of sulfur and metals, increasing metasomatic enrichment of the mantle wedge with volatile substances and large-ion lithophile elements* .

6. MAIN CONCLUSIONS

1. It has been established that during the formation of eight large and giant Cu-porphyry deposits of the Pacific belt, the rate of change in the angle of convergence in the horizontal plane increases in the zone of interaction between two tectonic plates. At the same time, the absolute convergence rate can either decrease or increase.

2. According to geological, structural, and kinematic data, supra-subduction magmatism, which resulted in the formation of 8 large and giant Cu-porphyry deposits, was accompanied by through-crustal disjunctive disturbances associated either with the change from frontal convergence (orthogonal convergence) to "oblique convergence" (Corbett, Leach, 1997; and many others), or with the transition to a transform continental margin regime (Khanchuk et al., 2019; Petrov et al., 2021; and others), or with a reversive change in the direction of subduction related to island arc - continent collision, island arc - oceanic plateau collision. All of the above geodynamic settings imply the presence of major deep faults, including transform faults.

3. Statistical analysis of the time series of Cu-porphyry deposits in the Pacific belt and their total ore volume formed in the last 125 million years showed the presence of a (quasi)cyclic component with a period of 26-28 million years, whose share in the total amplitude is 74%.

4. An inverse correlation has been established between the global spreading rate (Boulila et al., 2021; Muller et al., 2019), on the one hand, and the number of Cu-porphyry deposits in the Pacific belt and their productivity, on the other hand, for the last 125 million years. Moreover, the relative minimums of the spreading rate precede the relative maximums of the number and total volume of Cu-porphyry deposits by 5-10 million years. Perhaps during this time, there was a restructuring of plate kinematics, shifts appeared, and magmas broke through to the surface.

ACKNOWLEDGMENTS

The authors express their gratitude to A.I. Khanchuk for discussing this research topic, valuable comments and suggestions, as well as to I.V. Vikentyev and two anonymous reviewers, most of whose comments were taken into account when preparing the final version of the work.

FUNDING

The work was carried out with the support of the Russian Science Foundation grant (project No. 22-17-00023). Basic funding was provided by subsidies for state assignments of GIN RAS (theme No. FMMG-2023-0010) and ITIG FEB RAS (research themes No. 121021000095-1, No. 121021000094-4).

REFERENCES

Arkhipov M.V., Voinova I.P., Kudymov A.V., Peskov A.Yu., Oto Sh., Nagata M., Golozubov V.V., Didenko A.N. Comparative analysis of Aptian-Albian rocks from the Kema and Kiselevka-Manoma terranes: geochemistry, geochronology, and paleomagnetism // Pacific Geology. 2019. Vol. 38. No. 3. P. 58–83.

Bukhanova D.S. Mineralogical and geochemical features of the Malmyzh gold-copper porphyry deposit, Khabarovsk Territory: abstract of dissertation Cand. Geol.-Min. Sciences: 25.00.11. Petropavlovsk-Kamchatsky, 2020. 25 p.

Vikentiev I.V., Bortnikov N.S. Preface to the special issue of the journal "Geology of Ore Deposits" dedicated to porphyry and related deposits of Northern Eurasia // Geology of Ore Deposits. 2023. Vol. 65. No. 7. P. 591-595. DOI: 10.31857/S0016777023070067

Vikentiev I.V., Bortnikov N.S. Preface to the special issue of the journal "Geology of Ore Deposits" dedicated to porphyry and related deposits of Northern Eurasia // Geology of Ore Deposits. 2024. Vol. 66. No. 1. P. 3-6.

Volkov A.V., Sidorov A.A., Starostin V.I. Metallogeny of volcanogenic belts and activation zones. Moscow: MAKS Press, 2014. 356 p.

Geodynamics, Magmatism, and Metallogeny of the East of Russia: in 2 books / Ed. by A.I. Khanchuk. Vladivostok: Dalnauka. 2006. Book 1, 572 p., Book 2, 409 p.

State Geological Map of the Russian Federation. Scale 1:1,000,000 (third generation). Far East Series. Sheet M-53 – Khabarovsk. Explanatory note. St. Petersburg: VSEGEI Map Factory, 2009. 376 p.

Didenko, A.N., Arkhipov, M.V., Taltykin, Yu.V., Krutikova, V.O., Konovalova E.A. Petro-paleomagnetic characteristics of gabbrodiorites of the Lower Amur complex of the Zhuravlevka-Amur terrane (Sikhote-Alin orogenic belt) // Pacific Geology. 2023. Vol. 42. No. 5. P. 57–75. doi: 10.30911/0207-4028-2023-42-5-57-75

Dobretsov N.L. Ore formation and global geological processes: evolution and problems of periodicity / Smirnov Collection-96: main problems of ore formation and metallogeny. Moscow, 1996. P. 38–60.

Davis J.S. Statistical analysis of data in geology. Transl. from English. In 2 books/Transl. by V.A. Golubeva. Ed. by D.A. Rodionov. Moscow: Nedra, 1990. Book 1 (319 p.). Book 2 (427 p.).

Kalambet Yu.A., Kozmin Yu.P., Samokhin A.S. Noise filtering. Comparative analysis of methods // Analytics. 2017. Vol. 36. No. 5. P. 88-101. DOI: 10.22184/2227-572X.2017.36.5.88.101

Cox A., Hart R. Plate Tectonics. Moscow: Mir, 1989. 427 p.

Lyubushin A.A. Data analysis of geophysical and environmental monitoring systems. Moscow: Nauka, 2007. 228 p.

Rundkvist D.V., Tkachev A.V., Cherkasov S.V., Gatinsky Yu.G., Vishnevskaya N.A. Database and metallogenic map of large and super-large deposits of the world: principles of compilation and preliminary analysis of results / Large and super-large deposits: patterns of location and conditions of formation. Ed. by D.V. Rundkvist. Moscow: IGEM RAS, 2004. P. 391–422.

Khanchuk A.I., Ivanov V.V., Ignatiev E.K., Kovalenko S.V., Semenova D.V. Albian-Cenomanian magmatism and copper ore genesis of Sikhote-Alin // Doklady RAS. 2019. Vol. 488. No. 3. P. 69–73.

Sharapov V.N., Lapukhov A.S., Smolyaninova L.G. Temporal characteristics of the development of volcano-plutonic ore-magmatic systems of the Pacific margins // Geology and Geophysics. 2013. Vol. 54. No. 11. P. 1731–1753.

Yakubchuk A.S. Porphyry deposits of Northern Eurasia: practical aspects of tectonic control, structural features, and erosion level assessment from the Urals to the Pacific Ocean // Geology of Ore Deposits. 2024. Vol. 66. No. 1. P. 7–26.

Amilibia A., Sabat F., McClay K.R., Munoz J.A., Roca E., Chong G. The role of inherited tectono-sedimentary architecture in the development of the central Andean mountain belt: Insights from the Cordillera de Domeyko // J. Struct. Geol. 2008. V. 30(12). P. 1520–1539. doi:10.1016/j.jsg.2008.08.005

Argus D.F., Gordon R.G., DeMets C. Geologically current motion of 56 plates relative to the no-net-rotation reference frame // Geochem. Geophys. Geosyst. 2011. V. 12. Q11001. doi:10.1029/2011GC003751.

Boulila S., Haq B.U., Hara N., Müller R.D., Galbrun B., Charbonnier G. Potential encoding of coupling between Milankovitch forcing and Earth's interior processes in the Phanerozoic eustatic sea-level record // Earth-Science Reviews. 2021. V. 220. P. 103727(1–50). DOI:https://doi.org/10.1016/j.earscirev.2021.103727

Cao X., Zahirovic S., Li S., Suo Y., Wang P., Liu J., Müller R.D. A deforming plate tectonic model of the South China Block since the Jurassic // Gondwana Research. 2022. V. 102. P. 3-16. https://doi.org/10.1016/j.gr.2020.11.010

Cloos M., Sapiie B., van Ufford A.Q., Weiland R.J., Warren P.Q., McMahon T.P. Collisional

delamination in New Guinea: The geotectonics of subducting slab breakoff // Geological Society of America. Special Paper 400. 2005. 51 p. DOI: 10.1130/2005.2400

Coe R.S., Globerman B.R., Plumley P.W., Thrupp G. A. Paleomagnetic results from Alaska and their tectonic implications / In: Tectonostratigraphic Terranes of the CircumPacific Region, Ed. D.G. Howell. Am. Assoc. Petrol. Geol., Houston Circum-Pacific Council for Energy and Mineral Resources, Series 1. 1985. P. 85–108.

Coleman P.J., Hackman B.D. Solomon Islands / In Mesozoic-Cenozoic Orogenic Belts: Data for Orogenic Studies. Ed. by A.M. Spencer. Scottish Academic Press, Edinburgh, 1974. P. 453–461.

https://doi.org/10.1144/GSL.SP.2005.004.01.28

Cooke D.R., Hollings P., Walshe J.L. Giant Porphyry Deposits: Characteristics, Distribution, and Tectonic Controls // Economic Geology. 2005. V. 100. № 5. P. 801–818. 10.2113/gsecongeo.100.5.801.

Corbett G., Leach T. Southwest Pacific Rim Gold-Copper Systems: Structure, Alteration, and Mineralization // Economic Geology. Society of Economic Geologists. 1998. Special Publication 6. 238 p. DOI: 10.5382/SP.06Corpus ID: 112266656

Deng J., Yang X., Zhang Z-F., Santosh M. Early Cretaceous arc volcanic suite in Cebu Island, Central Philippines and its implications on paleo-Pacific plate subduction: Constraints from geochemistry, zircon U-Pb geochronology and Lu-Hf isotope // Lithos. 2015. V. 230. P. 166–179. https://doi.org/10.1016/j.lithos.2015.05.020

Diaz-Rodriguez J., Muller R. D., Chandrall R. Predicting the emplacement of Cordilleran porphyry copper systems using spatio-temporal machine learning model // Ore Geol. Rev. 2021. V. 137. 104300. https://doi.org/! 0.1016/j.oregeorev.2021.104300

Eastoe C.J. The formation of the Panguna porphyry copper deposit, Bbougainville, Papua New Guinea. Bachelor of Science (Honours). University of Tasmania, Hobart. 1979. 84 p.

English J.M., Jonston S.T. The Laramide Orogeny: What Were the Driving Forces? // International Geology Review. 2004. V. 46. P. 833–838.

Geological map, Bougainville and Buka Islands, Territory of Papua and New Guinea / compiled by Y. Miezitis. 1967. https://nla.gov.au/nla.obj-1532817321/view

GPlates software. 2022. https://www.gplates.org/

Hackman, B. D. 1980. The Geology of Guadalcanal, Solomon Islands. Overseas Memoir, Institute of Geological Sciences. London: 1980. № 6. 115 p.

Haeussler P.J., Saltus R.W. Twenty-six kilometers of offset since late Eocene time on the Lake Clark fault / In Haeussler P.J., Galloway J.P., eds. Studies by the U.S. Geological Survey in Alaska, 2004: U.S. Geological Survey Professional Paper 1709-A. 2005. P. 1–4.

Hammer O., Harper D.A.T., Ryan P.D. PAST: Paleontological Statistics software package for education and data analysis // Palaeontologia Electronica. 2001. V. 4. Is. 1. P. 1–9. https://palaeo-electronica.org/2001_1/past/past.pdf

Humphreys E., Hessler E., Dueker K., Farmer G. L., Erslev E., Atwater, T. How Laramide-Age Hydration of North American Lithosphere by the Farallon Slab Controlled Subsequent Activity in the Western United States // International Geology Review. 2003. V. 45(7). P. 575–595. https://doi.org/10.2747/0020-6814.45.7.575

Kay, S.M., Mpodozis C., Central Andean Ore Deposits Linked to Evolving Shallow Subduction Systems and Thickening Crust, GSA Today, 2001, 4(3), 4–9. doi:10.1130/1052-5173(2001)011<0004:caodlt>2.0.co;2

Khanchuk A.I., Kemkin I.V., Kruk N.N. The Sikhote-Alin orogenic belt, russian south east: terranes and the formation of continental lithosphere based on geological and isotopic data // Journal of Asian Earth Sciences. 2016. V. 120. P. 117–138.

Lang J.R., Gregory M.J. Chapter 8. Magmatic-Hydrothermal-Structural Evolution of the Giant Pebble Porphyry Cu-Au-Mo Deposit with Implications for Exploration in Southwest Alaska / Geology and Genesis of Major Copper Deposits and Districts of the World: A Tribute to Richard H. Sillitoe, Jeffrey W. Hedenquist, Michael Harris, Francisco Camus 2012 Society of Economic Geologists, Inc. 2012. P. 167–185.

Lang J.R., Gregory M.J., Rebagliati C.M., Payne J.G., Oliver J.L., Roberts K. Geology and magmatic-hydrothermal evolution of the giant Pebble porphyry copper-gold-molybdenum deposit, southwest Alaska // Economic geology. 2013. V. 108. P. 437–462.

Langton, J.M., Williams, S.A., Structural, petrological and mineralogical controls for the Dos Pobres orebody: Lone Star mining district, Graham County, Arizona (USA). Advances in geology of the porphyry copper deposits: southwestern North America, 1982, 335–352.

Li M., Hinnov L.A., Kump L.R. Acycle: Time-series analysis software for paleoclimate projects and education // Computers & Geosciences. 2019. V. 127. P. 12–22. https://doi.org/10.1016/j.cageo.2019.02.011

Liu, L., Gurnis, M., Seton, M. et al. The role of oceanic plateau subduction in the Laramide orogeny. Nature Geoscience. 2010. V. 3. P. 353–357. https://doi.org/10.1038/ngeo829

Lomb N.R. Least-squares frequency analysis of unequally spaced data // Astrophys. & Space Sci. 1976. V. 39. P. 447–462.

Maksaev, V., Munizaga, F., McWilliams, M., Fanning, M., Marther, R., Ruiz, J., Zentilli, M. Chronology for El Teniente, Chilean Andes, from U-Pb, 40Ar/39Ar, Re-Os, and fission track dating: implications for the formation of a supergiant porphyry Cu-Mo deposit. In: Sillitoe, R. H., Perello, J. & Vidal, C. E. (eds) Andean Metallogeny: New Discoveries, Concepts and Updates. Society of Economic Geologists, 2004, Special Publications 11, 15–54.

Mars J.C., Robinson G.R., Hammarstrom J.M., Zürcher L., Whitney H., Solano F., Gettings M., Ludington S. Porphyry Copper Potential of the United States Southern Basin and Range Using ASTER Data Integrated with Geochemical and Geologic Datasets to Assess Potential Near-Surface Deposits in Well-Explored Permissive Tracts // Economic Geology. 2019. V. 114 (6). P. 1095–1121. doi: https://doi.org/10.5382/econgeo.4675

Mihalasky M.J., Ludington S., Alexeiev D.V., Frost T.P., Light T.D., Briggs D.A., Hammarstrom

J.M., Wallis J.C., with contributions from Bookstrom A.A. and Panteleyev A. Porphyry copper assessment of Northeast Asia-Far East Russia and Northeasternmost China. U.S. Geological Survey, Scientific Investigations Report 2010-5090-W. 2015. 104 p., and spatial data. http://dx.doi.org/10.3133/sir20105090W

Mineral Resources Online Spatial Data. 2023. https://mrdata.usgs.gov/#mineral-resources

Mpodozis C., Cornejo P. Chapter 14. Cenozoic Tectonics and Porphyry Copper Systems of the Chilean Andes / Geology and Genesis of Major Copper Deposits and Districts of the World: A Tribute to Richard H. Sillitoe, Jeffrey W. Hedenquist, Michael Harris, Francisco Camus 2012 Society of Economic Geologists, Inc. 2012. P. 329–360.

Müller R.D., Zahirovic S., Williams S.E., Cannon J., Seton M., Bower D.J., Tetley M.G., Heine C., Le Breton E., Liu S., Russell S.H.J., Yang T., Leonard J., Gurnis M. A global plate model including lithospheric deformation along major rifts and orogens since the Triassic // Tectonics. 2019. V. 38(6) P. 1884–1907. https://doi.org/10.1029/2018TC005462

Nagel T.J., Ryan W.B.F., Malinvemo A., Buck W.R. Pacific trench motions controlled by the asymmetric plate configuration // Tectonics. 2008. V. 27. TC3005. doi:10.1029/2007TC002183, 2008

Olson, N., Dilles, J.H., Kent, A.J.R., Lang, J.R., Geochemistry of the Cretaceous Kaskanak batholith and genesis of the pebble porphyry Cu–Au–Mo deposit, southwest Alaska. American Mineralogist, 2017, 102, 1597–1621, https://doi.org/10.2138/am-2017-6053

Ossandon G., Freraut R., Gustafson L.B., Lindsay D.D., Zentilli, M. Geology of the Chuquicamata mine: A progress report // Economic Geology. 2001. V. 96. P. 249–270.

Page R.W., McDougall I. Geochronology of the Panguna porphyry copper deposit, Bougainville Island, New Guinea // Economic Geology. 1972. V. 67(8). P. 1065–1074.

Paterson J.T., Cloos M. Grasberg porphyry Cu-Au deposit, Papua, Indonesia: 1. Magmatic history / In Super Porphyry Copper & Gold Deposit: A Global Perspective. Ed. T.M. Porter. Adelaide: PGC Publishing, 2005. V. 2. P. 313–329.

Petrov O.V., Khanchuk A.I., Ivanov V.V., Shatov V.V., R. Seltmann C., Dolgopolova A.V., Alenicheva A.A., Molchanov A.V., Terekhov A.V., Leontev V.I., Belyatsky B.V., Rodionov N.V., Sergeev S.A. Porphyry indicator zircons (PIZ) and geochronology of magmatic rocks from the Malmyzh and Pony Cu-Au porphyry ore fields (Russian Far East) // Ore Geology Reviews. 2021. V. 139. Article 104491. https://doi.org/10.1016/j.oregeorev.2021.104491

Pisarevsky, S.A., Li, Z.X., Tetley, M.G., Liu, Y., Beardmore, J.P., An updated internet-based Global Paleomagnetic Database, Earth-Science Reviews, Volume 235, 2022, 104258, https://doi.org/10.1016/j.earscirev.2022.104258.

Prokoph A., Fowler A.D., Patterson R.T. Evidence for periodicity and nonlinearity in a highresolution fossil record of long-term evolution // Geology. 2000. V. 28. P. 867–870.

Ramos V.A., Folguera A. Andean flat-slab subduction through time / Ancient Orogens and Modern Analogues, eds.: Murphy J.B., Keppie J.D., Hynes A. J. Geological Society, London. 2009. Special

Publications. V. 327. P. 31–54. DOI: 10.1144/SP327.3 0305-8719/09

Ramos V.A., Folguera A., Payenia volcanic province in the Southern Andes: An appraisal of an exceptional Quaternary tectonic setting, J.Volcanology&Geothermal Res. 2011, 201, 53–64. doi:10.1016/j.jvolgeores.2010.09.008

Rampino M.R., Caldeira K., Zhu Y. A 27.5-My underlying periodicity detected in extinction episodes of non-marine tetrapods // Historical Biology. 2021a. V. 33(11). P. 3084–3090. DOI: 10.1080/08912963.2020.1849178

Rampino M.R., Caldeira K., Zhu Y. A pulse of the Earth: A 27.5-Myr underlying cycle in coordinated geological events over the last 260 Myr // Geoscience Frontiers. 2021b. Volume 12, Issue 6, 101245. https://doi.org/10.1016/j.gsf.2021.101245.

Raup D.M., Sepkoski J.J. Periodicity of extinctions in the geologic past // Proceedings of the National Academy of Sciences. 1984. V. 81. No. 3. P. 801–805. doi:10.1073/pnas.81.3.801. PMC 344925. PMID 6583680.

Richards J.P . Porphyry copper deposit formation in arcs: What are the odds? // Geosphere. 2021. V. 18(1). P. 130–155. https://doi.org/10.1130 /GES02086.1

Richards J.P. Postsubduction porphyry Cu-Au and epithermal Au deposits: Products of remelting of subduction-modified lithosphere // Geology. 2009. V. 37. P. 247–250.

Rodrigo J.D., Gabo-Ratio J.A.S., Queaño K.L., Fernando A.G.S., de Silva L.P., Yonezu K., Zhang Y. Geochemistry of the Late Cretaceous Pandan Formation in Cebu Island, Central Philippines: Sediment contributions from the Australian plate margin during the Mesozoic // Depositional Rec. 2020. 6. P. 309–330. https://doi.org/10.1002/dep2.103

Russin D ., (2008) Hypogene alteration and mineralization in the Dos Pobres porphyry Cu (-Au-Mo) deposite, Safford district, Arizona: a gold -and magnetite-rich variant of Arizona porphyry copper systems. A thesis submitted to the faculty of the department of geosciences, 2008, 120 p. www.geo.arizona.edu/Antevs/Theses/RussinMS08.pdf

Sapiie B, Cloos M. Strike-slip faulting in the core of the Central Range of west New Guinea:

Ertsberg Mining District, Indonesia // Geological Society of America Bulletin. 2004. V. 116. P.

277–293.

Sapiie B. Kinematic Analysis of Fault-Slip Data in the Central Range of Papua, Indonesia // Indonesian Journal on Geoscience. 2016. V. 3 (1). P. 1–16. DOI:10.17014/ijog.3.1.1-16

Savitzky A., Golay M.J.E. Smoothing and Differentiation of Data by Simplified Least Squares Procedures // Anal. Chem. 1964. V. 36. P. 1627–1639. doi:10.1021/ac60214a047

Scargle J.D. Studies in astronomical time series analysis. II. Statistical aspects of spectral analysis of unevenly spaced data // Astrophys. J. 1982. Vol. 263. P. 835–853.

Sillitoe R.H. Chapter 1. Copper Provinces / Geology and Genesis of Major Copper Deposits and Districts of the World: A Tribute to Richard H. Sillitoe, Jeffrey W. Hedenquist, Michael Harris, Francisco Camus 2012 Society of Economic Geologists, Inc. 2012. P. 1–-18.

Sillitoe R.H. Porphyry copper systems // Economic Geology. 2010. V. 105. P. 3–41. https://doi.org/10.2113/gsecongeo.105.1.3.

Singer D.A., Berger V.I., Moring B.C. Porphyry Copper Deposits of the World: Database And Grade and Tonnage Models, 2008. Open-File Report 2008-1155. U.S. Geological Survey, Menlo Park. 2008. 46 p. https://www.researchgate.net/publication/303172164_Porphyry_ copper_deposits_of_the_world_database_map_grade_and_tonnage_models/link/5f530c17299bf13a 31a0946e/Stern, C.R., Skewes, M.A., Arevalo A., Magmatic Evolution of the Giant El Teniente Cu–Mo Deposit, Central Chile, J.Petrology, 2011, 52(7&8), 1591–1617.

Taylor B. A Geophysical Survey of the WoodlarkSolomons Region. Circum-Pacific Council for Energy and Mineral Resources, Earth Sci. 1987. Ser. 7. P. 25–48.

Zhou D., Li CF., Zlotnik S., Wang J. Correlations between oceanic crustal thickness, melt volume, and spreading rate from global gravity observation // Mar Geophys Res. 2020. V. 41. №. 14 (2020). https://doi.org/10.1007/s11001-020-09413-x

Table 1. Position and kinematic characteristics at the time of formation of the eight largest Cu-porphyry deposits in the Pacific belt

deposit (tectonic setting)	latitude, deg.	longitude, deg.	age, million years	ore mass million tons,	subducting plate	obducting plate	change in convergence rate, deg./million years	change in convergence angle, deg.	geodynamic setting
Atlas island arc	10.37 (-5.5)	123.83 (127.5)	108.0	1420	Izanagi ↔Philippine		1.38–1.08 (-0.30)	140–90 (+50)	oblique subduction + arc-continent collision + subduction inversion
Malmyzh mixed	49.92 (64.7)	136.90 (122.6)	97.0	2400	Izanagi	Eurasian (Amur)	0.92–1.30 (+0.38)	342–333 (+9)	oblique subduction-transform + arc-continent collision
Pebble continental margin	59.90 (73.4)	-155.30 (-105.2)	89.5	7510	Farallon	North American	1.27–1.38 (+0.11)	80–50 (+30)	oblique subduction + mid-ocean ridge subduction
Safford continental margin	32.93 (36.4)	-109.60 (-97.8)	52.5	7260	Vancouver	North American	0.88–1.30 (+0.42)	35–65 (-30)	end of flat subduction + plateau subduction
Chuquicamata continental margin	-22.27 (-27.1)	-68.90 (-67.5)	33.0	21277	Farallon	South American	1.65–1.35 (-0.30)	65–75 (-10)	flat subduction
El Teniente continental margin	-34.09 (-34.6)	-70.46 (-70.4)	5.4	20731	Nazca	South American	1.03–0.93 (-0.10)	87–77 (+10)	end of flat subduction + oblique subduction + ridge subduction
Panguna island arc	-6.32 (-6.7)	155.50 (157.2)	3.4	1420	Pacific ↔Australian		1.10–1.09 (-0.01)	257–250 (+7)	arc-oceanic plateau collision + subduction inversion
Grasberg postconvergence	-3.82 (-5.4)	137.23 (136.4)	3.0	4000	Caroline ↔Australian		1.04–1.91 (+0.87)	295–210 (+85)	oblique subduction + arc-continent collision + subduction inversion

Note. Tectonic setting during deposit formation (coordinates, age, and ore mass are given according to (Mihalasky et al., 2015; Mineral Resources..., 2023; Singer et al., 2008); in the "latitude" and "longitude" columns, current coordinates (without brackets) and paleocoordinates at the time of deposit formation (in brackets) are shown; in the "subducting plate" and "obducting plate" columns, the sign ↔ for Panguna and Grasberg deposits indicates a change in subduction direction (see explanations in the text); in the "convergence angle change" column, the signs "+" and "-" indicate counterclockwise and clockwise rotation, respectively.

Fig. 1. Location of copper porphyry deposits worldwide (a) and in the Pacific belt with ore volume exceeding 1 million tons (b)

(a): 1 – Cu-porphyry deposits worldwide according to (Mihalasky et al., 2015; Mineral Resources…, 2023; Singer et al., 2008); 2 – major cities. Equal-area projection, central meridian 150°.

(b): 1 – tectonic plate boundaries according to (Bird, 2003; Argus et al., 2011), plate names are given in italics: Altiplano, Amur, Antarctica, Australia, Banda, Birds head, Caribbean, Caroline, Cocos, Easter, Eurasia, Juan de Fuca, Juan Fernandez, Kermadec, Malucca, Maoke, Mariana, N.America, N.Andes, N.Bismarck, Nazca, New Hebrides, Okhotsk, Okinava, Pacific, Panama, Philippine, Rivera, S.America, S.Bismarck, Scotia, Solomon, Sunda, Timor, Tonga, Woodlark, Yangtze; 2 – deposit locations indicating age group (color) and total ore quantity (size) according to (Singer et al., 2008; Mihalasky et al., 2015); 3 – locations of the largest Cu-porphyry deposits in their age group: 1 – Atlas, 2 – Malmyzh, 3 – Pebble Copper, 4 – Safford, 5 – Chuquicamata, 6 – El Teniente, 7 – Panguna, 8 – Grasberg. Equal-area projection, central meridian 210°.

Fig. 2. Distribution of Cu-porphyry deposits in the Pacific belt by time (a) and by volume (b), time dependence of the total ore volume of all deposits in the Pacific belt (c).

In (b), the solid line shows the theoretical lognormal distribution with statistical parameters similar to the observed data. In (c), the bar chart shows the original series and the dotted line shows the smoothed Savitzky-Golay filter (Savitzky, Golay, 1964).

Fig. 3. Analysis of the temporal dependence of the total volume of ore from Cu-porphyry deposits in the Pacific Belt over the past 125 million years.

(a) – the original series is shown by a bar histogram, the dashed line represents the series smoothed with the Savitzky-Golay filter (Savitzky, Golay, 1964).

(b) – autocorrelation functions (Davis, 1990) of the original series (solid line) and smoothed series (dashed line).

(c), (d) – Lomb-Scargle periodograms (Baluev, 2009; Lomb, 1976; Scargle, 1982) of the original and smoothed series, respectively.

(e), (f) – Morlet Wavelet diagrams (Lyubushin, 2007; Torrence, Compo, 1998) of the original and smoothed series, respectively.

Fig. 4. Paleoreconstructions (a, c) and calculation of kinematic parameters (b, d) for 108 million years ago for the Atlas deposit and 95 million years ago for the Malmyzh deposit.

Legend for (a) and (c): 1–4 – boundaries of lithospheric tectonic plates according to (Bird, 2003; Argus et al., 2011) with additions and changes: 1 – divergent, 2 – convergent active (operating at the time of deposit formation), 3 – convergent extinct, 4 – transform; 5 – transform faults; 6 – direction and speed of lithospheric plate migration (arrow length proportional to speed); 7 – reconstructed positions of deposits. Abbreviations of tectonic plates in Fig. 4–7: ANT – Antarctic, AUS – Australian, CAR – Caroline, CEL – Celebes Basin, EHA – East Halmahera, EPH – East Philippine, ESP – Sunda, EUR – Eurasian, FAR – Farallon, NSW – North Sulawesi, IZA – Izanagi, MOL – Molucca, NAM – North American, NAZ – Nazca, NBA – North Banda, NBK – North Bismarck, NHB – New Hebrides, NTE – Neo-Tethys, NWB – North Woodlark, PAC – Pacific, PHS – Philippine, SAM – South American, SBA – South Banda, SBK – South Bismarck, SOL – Solomon Sea, SSW – South Sulawesi, VAN – Vancouver, WHA – West Halmahera, WOY – Woyla, index "b" means back-arc basin, WPH – West Philippine. In "c" the abbreviation CSAR means Central Sikhote-Alin Fault.

Legend for (b) and (d): circles – speed; triangles – azimuth.

Global reconstructions were used (Muller et al., 2019), as well as specific paleogeodynamic characteristics for "a" (Deng et al., 2015; McCabe et al., 1987; Rodrigo et al., 2019) and "c" (Arkhipov et al., 2019; Didenko et al., 2023; Khanchuk et al., 2016). Calculation of kinematic parameters in Fig. 4-7 was performed for the coordinates of deposits (see Table 1) using GPlates software (2022).

Fig. 5. Fragments of global reconstructions (a, c) and calculation of kinematic parameters (b, d) at 89 million years ago for the Pebble deposit and 52 million years ago for the Safford deposit.

For legend, see Fig. 4.

Global reconstructions were used (Muller et al., 2019), as well as specific paleogeodynamic characteristics for the Pebble deposits (Harris et al., 1987; Hillhoese, Gromme, 1988; Olson et al., 2017) and Safford (Hagstrum, 1994; Liu et al., 2010; Vugteveen et al., 1981).

Fig. 6. Fragments of global reconstructions (a, c) and calculation of kinematic parameters (b, d) at 33 million years ago for the Chuquicamata deposit and 5 million years ago for the El Teniente deposit.

For legend, see Fig. 4.

Global reconstructions were used (Muller et al., 2019), as well as specific paleogeodynamic characteristics for the Chuquicamata deposits (Prezzi, Vilas, 1998; Ramos, Folguera, 2009) and El Teniente (Goguitchaichvili et al., 2000; Ramos, Folguera, 2009; 2011).

Fig. 7. Fragment of global reconstruction (a) and calculation of kinematic parameters (b, c) at 3 million years ago for the Panguna and Grasberg deposits.

In (a), the black bold dotted line indicates the northern boundary of the overthrust Australian plate. GR - Grasberg deposit, PN - Panguna deposit. For other symbols, see Fig. 4.

Global reconstructions were used (Muller et al., 2019) taking into account data (Cloos et al., 2005; Sapiie, 2016), as well as specific paleogeodynamic characteristics for the Panguna deposits (Musgrave, 1990; Taylor, 1987) and Grasberg (Paterson, Cloos, 2005; paleomagnetic poles Nos. 1911, 1912 from Pisarevsky et al., 2022).

Fig. 8. Comparison of models (a) of spreading rate (Baulila et al., 2021; Muller et al., 2019) and (b) the total ore volume of Cu-porphyry deposits in the Pacific Belt (present work) for the last 125 million years.

Numbers of time dependencies on (a): 1, 2 – spreading rate of MOR according to (Müller et al. 2019) and its trend calculated by smoothing the original values, according to (Boulila et al., 2021), respectively; 3, 4 – model reconstructed time series of spreading rate after trend removal and the highest amplitude harmonic of the model series according to (Boulila et al., 2021), respectively.

Numbers of time dependencies on (b): 5, 6 – original series of total ore volume and smoothed by Savitzky-Golay filter (present work), respectively; 7, 8 – model reconstructed time series of total ore volume and the highest amplitude harmonic of the model series according to (present work), respectively.

Gray rectangles emphasize the temporal relationship between the maxima in the time dependencies of total ore volume (b), on the one hand, and minima in the time dependencies of spreading rate (a), on the other.

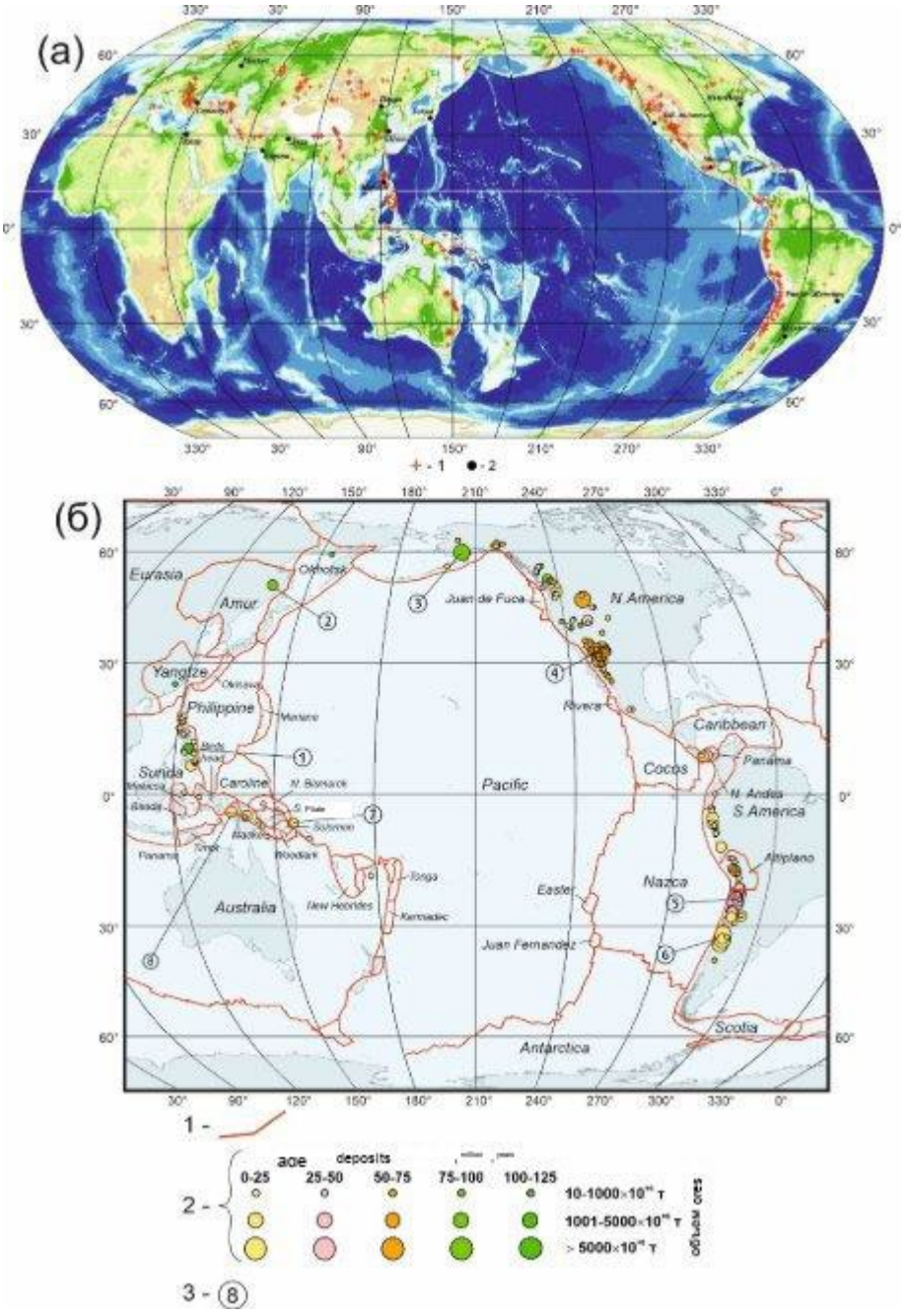

Fig. 1

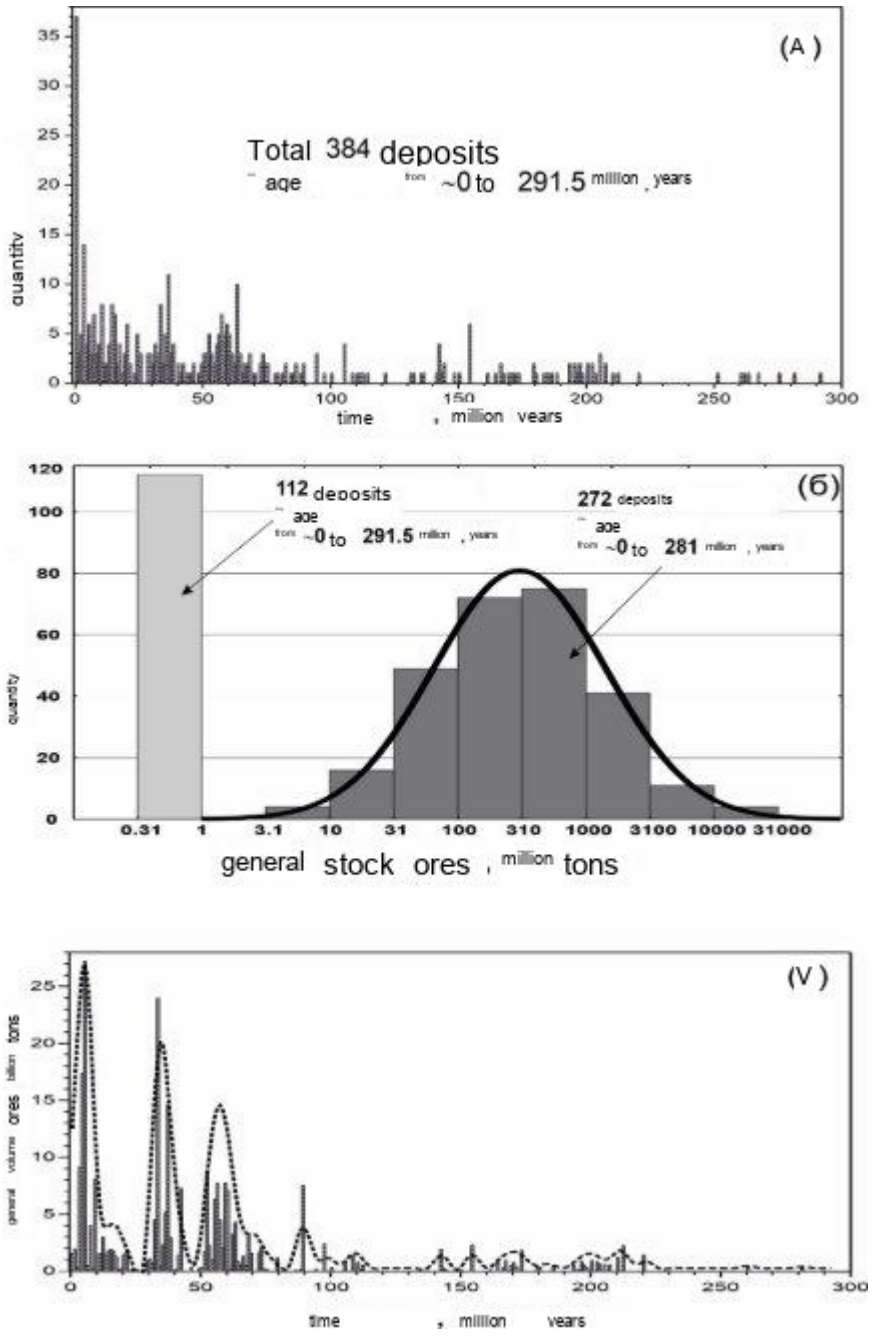
(А)
Total 384 deposits
age from ~0 to 291.5 million years
quantity
time, million years
(б)
112 deposits
age from ~0 to 291.5 million years
272 deposits
age from ~0 to 281 million years
quantity
0.31 1 3.1 10 31 100 310 1000 3100 10000 31000
general stock ores, million tons
(V)
general volume ores billion tons
time, million years

Fig. 2

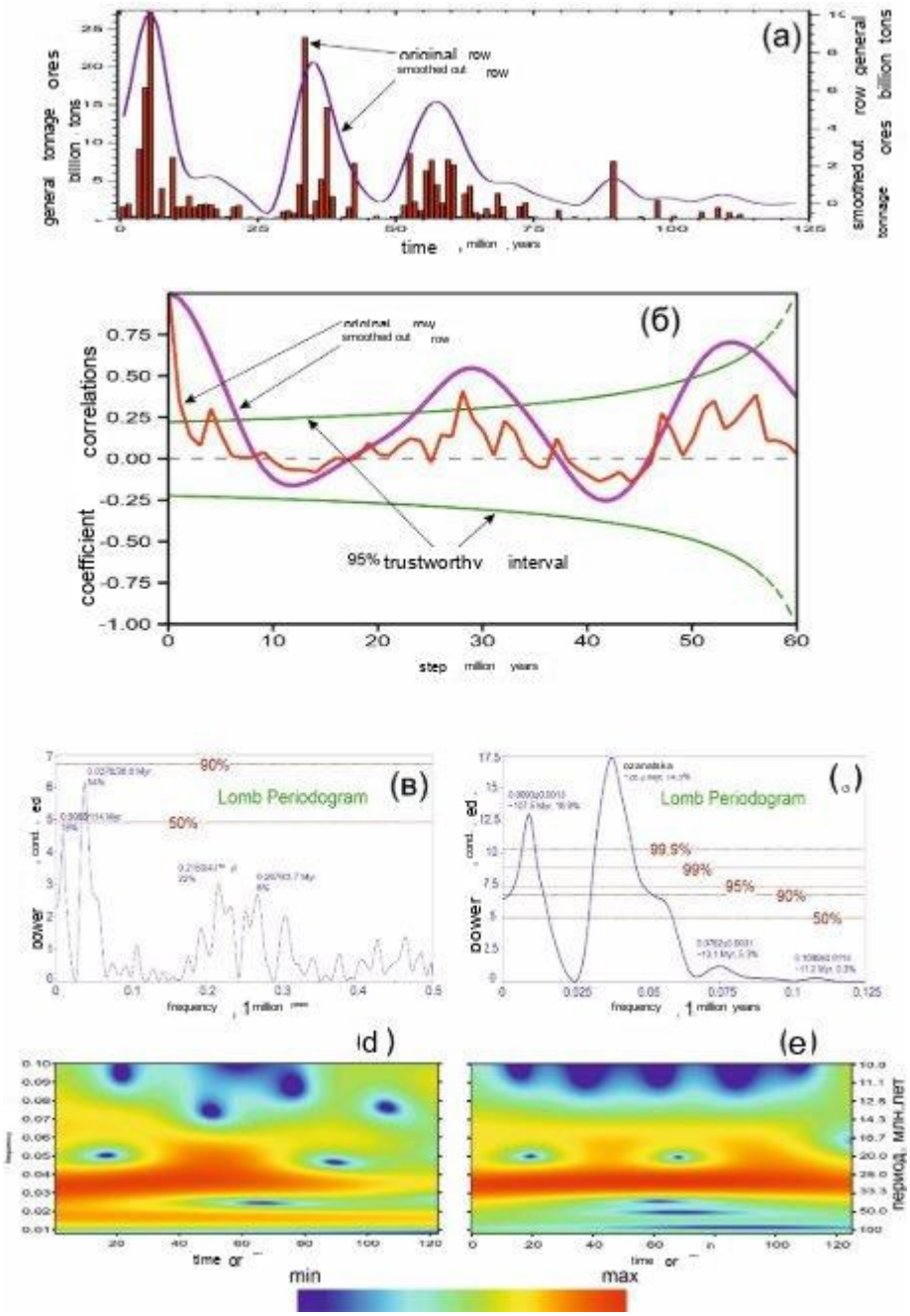
(a)
original row
smoothed out row
general tonnage ores billion . tons
smoothed out row general tonnage ores billion tons
time , million , years
(б)
correlations
coefficient
95% trustworthy interval
step million years
(в)
Lomb Periodogram
90%
50%
power
frequency , 1 million years
(г)
Lomb Periodogram
99.9%
99%
95%
90%
50%
power
frequency , 1 million years
(d)
(e)
time or
min
max
период, млн.лет

Fig. 3

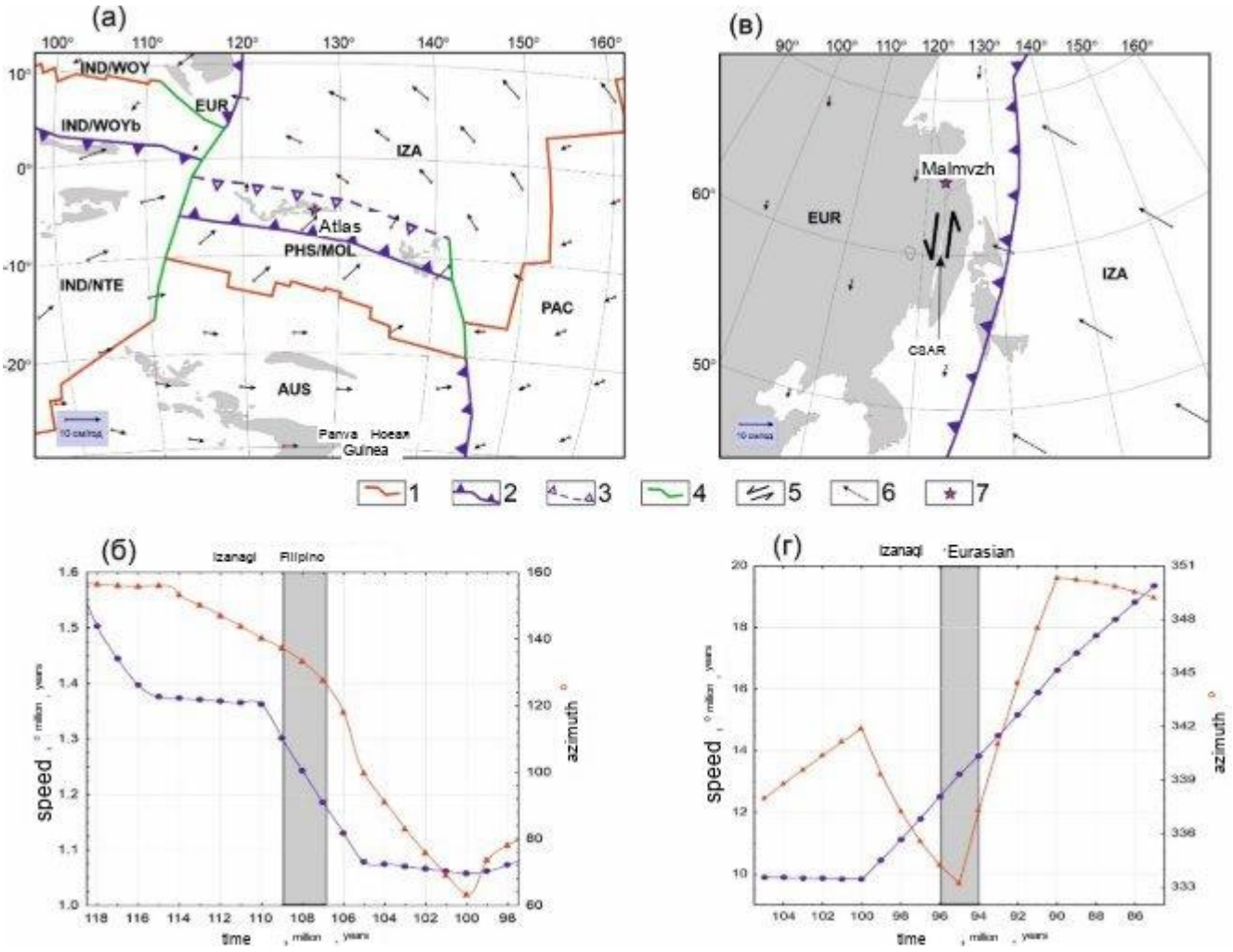
(а)
IND/WOY
EUR
IND/WOYb
IZA
Atlas
PHS/MOL
IND/NTE
PAC
AUS
Papua New Guinea
(в)
Malmyzh
EUR
IZA
CBAR
1
2
3
4
5
6
7
(б)
Izanagi
Pilipino
speed, ° million years
azimuth °
time, million years
(г)
Izanagi
Eurasian
speed, ° million years
azimuth °
time, million years

Fig. 4

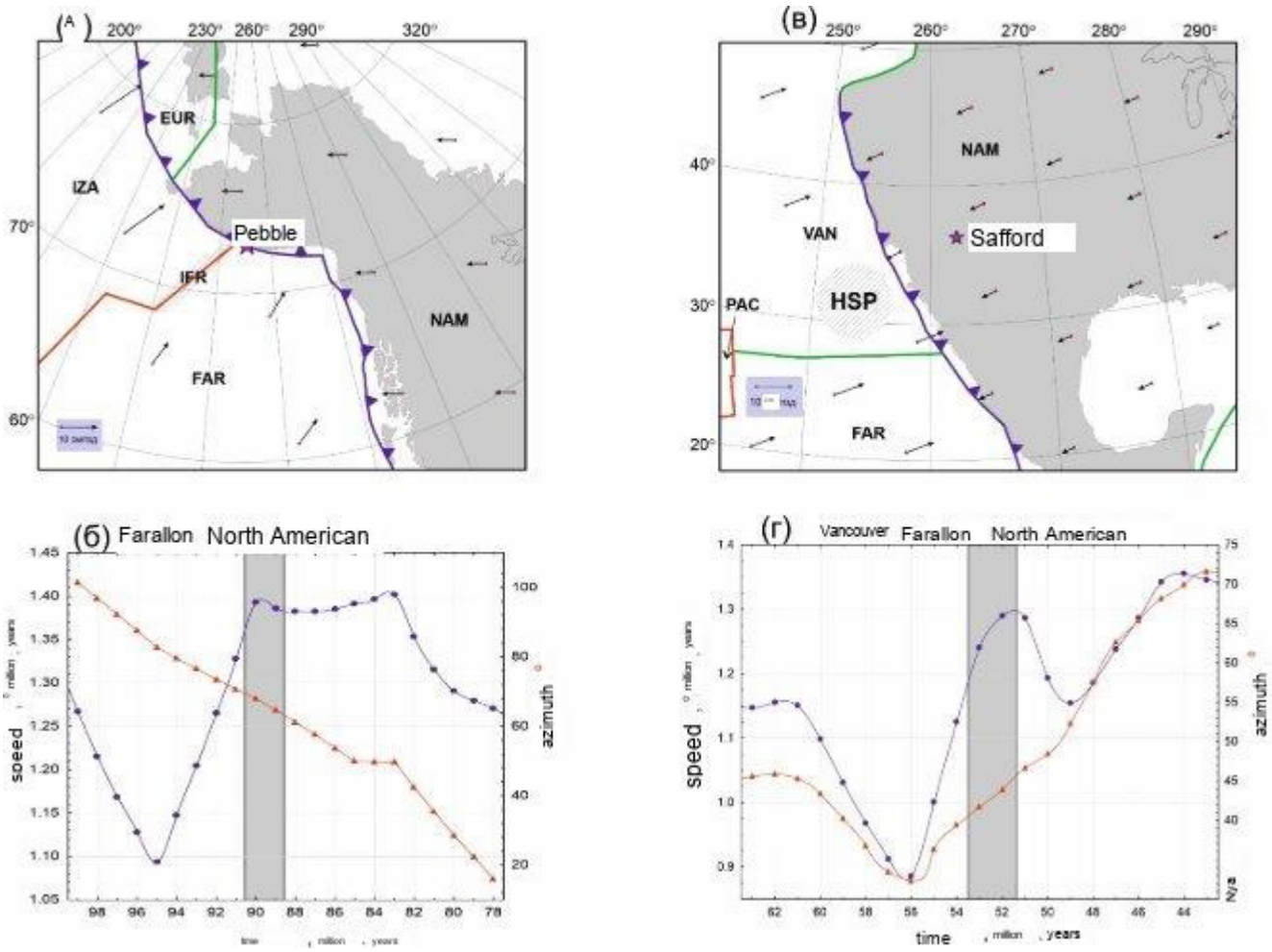
(А)
200°
230°
260°
290°
320°
70°
60°
EUR
IZA
Pebble
IFR
NAM
FAR
(В)
250°
260°
270°
280°
290°
40°
30°
20°
NAM
VAN
Safford
PAC
HSP
FAR
(б) Farallon North American
speed , ° million , years
azimuth
time , million , years
(г) Vancouver Farallon North American
speed , ° million , years
azimuth
N/a
time , million , years

Fig. 5

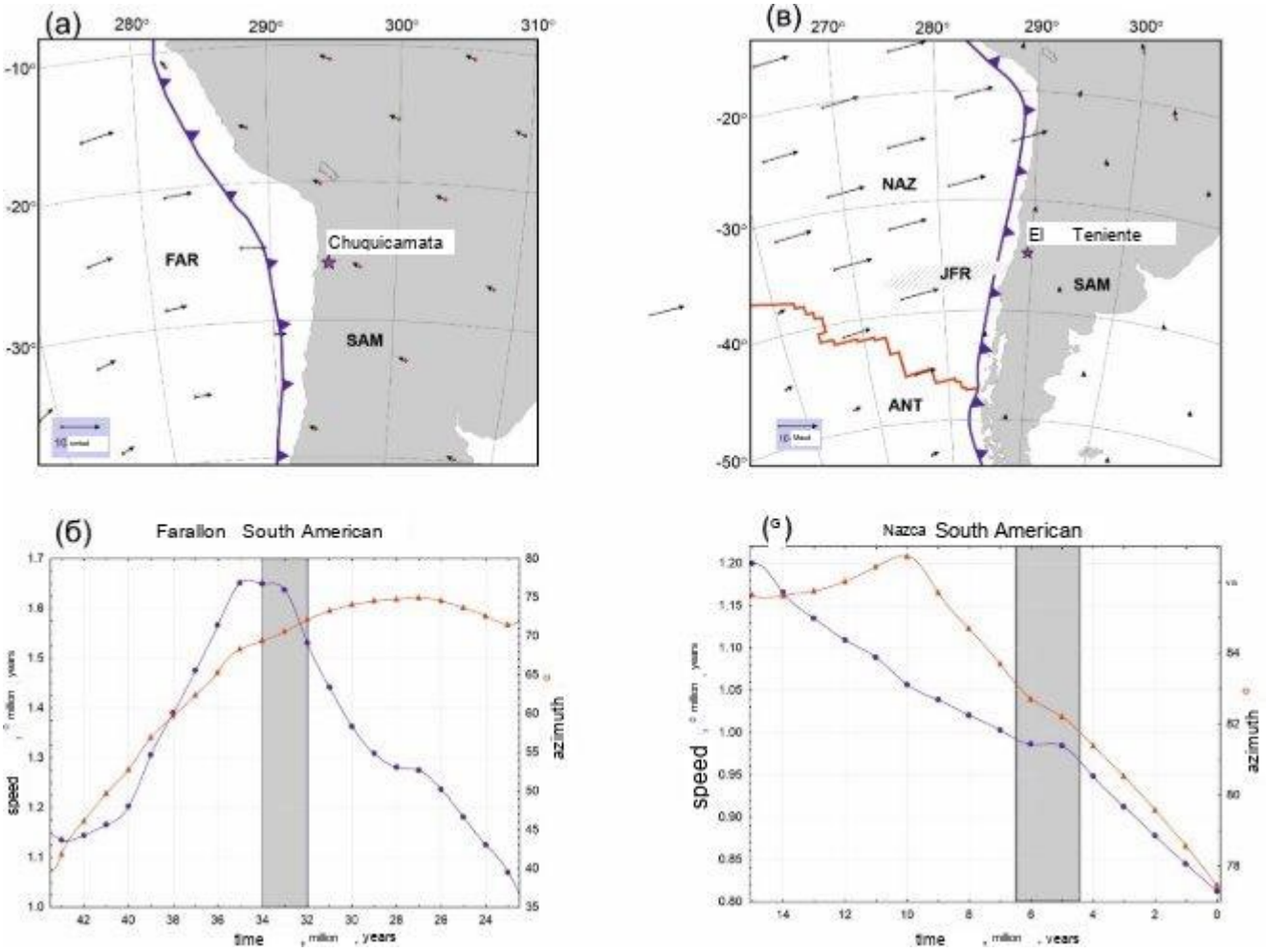
(а)
280°
290°
300°
310°
-10°
-20°
-30°
FAR
Chuquicamata
SAM
(в)
270°
280°
290°
300°
-20°
-30°
-40°
-50°
NAZ
El Teniente
JFR
SAM
ANT
(б)
Farallon South American
speed
azimuth
time
(г)
Nazca South American
speed
azimuth
time

Fig. 6

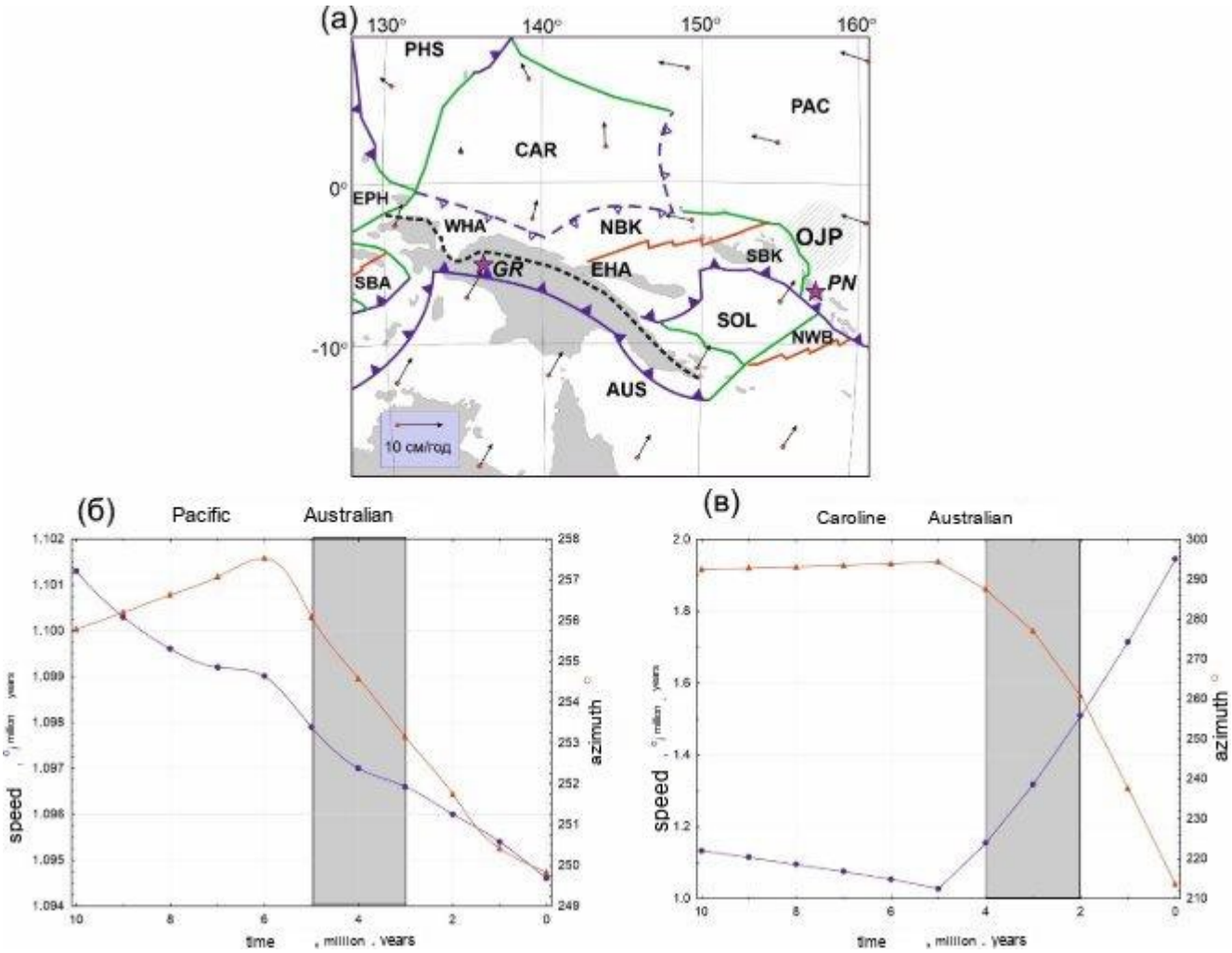
(а)
130°
140°
150°
160°
0°
-10°
PHS
PAC
CAR
EPH
WHA
NBK
OJP
SBK
GR
EHA
PN
SBA
SOL
NWB
AUS
10 см/год
(б)
Pacific
Australian
speed
azimuth
time
, million . years
(в)
Caroline
Australian
speed
azimuth
time
, million . years

Fig. 7

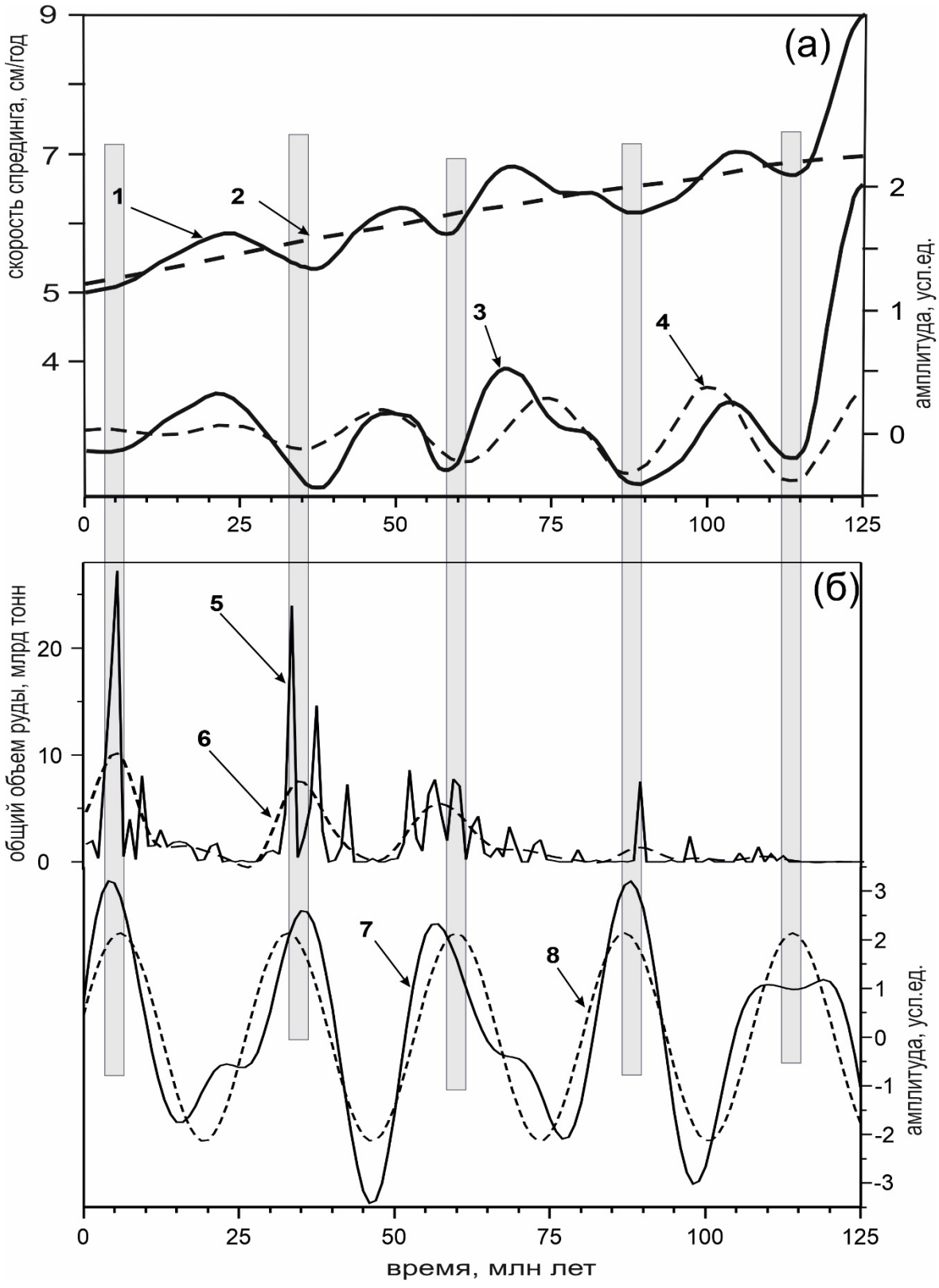
(а)
скорость спрединга, см/год
амплитуда, усл.ед.
1
2
3
4
(б)
общий объем руды, млрд тонн
амплитуда, усл.ед.
5
6
7
8
время, млн лет

Fig. 8